Available online at www.sciencedirect.com
SCIENCE DIRECT
Coordination Chemistry Reviews 250 (2006) 1332–1350
COORDINATION CHEMISTRY REVIEWS
www.elsevier.com/locate/ccr

Review

X-ray structural chemistry of cobalamins

Lucio Randaccio *, Silvano Geremia, Giorgio Nardin, Jochen Wuerges

Dipartimento di Scienze Chimiche, University of Trieste, 34127 Trieste, Italy

Received 6 July 2005; accepted 8 December 2005
Available online 3 February 2006

Contents

Abstract

In recent years, X-ray structural determinations of cobalamins (Cbl) have become very accurate thanks to the use of new detectors and synchrotron radiation. This has allowed in depth study of the geometrical features of cobalamins, regarding the large equatorial ligand and, more importantly, their axial fragment, which is involved in the binding of Cbl to proteins and in the catalytic mechanisms of Vitamin B_{12} based enzymes. These structural aspects, together with their particular crystal packing, are the focus of this review. Several chemical properties, derived from their structural chemistry and not reported in other reviews, are underlined. A comparison to the well-known simple Cbl model, the cobaloximes is also presented and discussed, as this furnishes useful insights into cobalamin chemistry.

Keywords: X-ray crystallography; Cobalamin; Cobaloxime; Vitamin B_{12}; B_{12}-enzyme model; *cis* and *trans* effect

Abbreviations: acacen, *N*,*N*′-bis-(aceylacetone)ethylendiimine; AdoCbl, 5′-deoxyadenosylcobalamin (coenzyme B_{12}); BDE, bond dissociation enthalpy; Bzm, 5,6-dimethylbenzimidazole; Cbl, cobalamin; DFT, density functional theory; DH, monoanion of dimethylglyoxime; E.S.D., estimated standard deviation; ESR, electron spin resonance; MD, molecular dynamics; MeCbl, methylcobalamin; MM, molecular mechanics; NMR, nuclear magnetic resonance; rms, root mean square; salen, *N*,*N*′-bis-(salicylaldehyde)-ethylendiimine

* Corresponding author. Tel.: +39 040 5583935; fax: +39 040 5583903.
E-mail address: randaccio@univ.trieste.it (L. Randaccio).

0010-8545/$ – see front matter © 2005 Elsevier B.V. All rights reserved.
doi:10.1016/j.ccr.2005.12.005

1. Introduction

Vitamin B_{12}, or cyanocobalamin (CNCbl), is not a biologically active species, whereas methylcobalamin (MeCbl) and 5′-deoxy-5′-adenosylcobalamin (B_{12} coenzyme, AdoCbl) (Fig. 1) are important as cofactors for L-methylmalonyl-CoA mutase and methionine synthase in both mammalians and prokaryotes, as well as for several other enzymes found exclusively in prokaryotes [1,2]. Cobalamins (Cbls) contain a Co atom equatorially coordinated by a corrin ring possessing seven amide side chains (*a*–*g*) (Fig. 1). Chain *f* connects through an amide bond to a nucleotide, whose benzimidazole base normally coordinates to Co at the axial position on the α side (lower side) of the corrin macrocycle (base-on form, Fig. 1a). In the Co(III) state, another axial ligand X is coordinated on the β side (upper side) of the equatorial plane.

Like most vitamins, cobalamin cannot be synthesized by higher organisms and it must be supplied with diet. Mammalians have developed a complex transportation mechanism (Fig. 2) with three binding proteins, haptocorrin (HC), intrinsic factor (IF) and transcobalamin (TC), for intestinal absorption, transport and cellular uptake of the vitamin [3].

The dietary Cbl is preferentially bound to salivary HC, which protects the vitamin from acid hydrolysis. Pancreatic proteases in the duodenum cleave HC and release Cbl, which then binds to gastric intrinsic factor, forming the complex IF-Cbl [4]. Inside the enterocytes, cobalamin is transferred from intrinsic factor to TC and transported into portal plasma, where the TC-Cbl complex is endocytosed by membrane receptors [5]. Inside the target cells, the cobalamin molecules are metabolized to the two cofactors: 5′-deoxyadenosyl-Cbl (coenzyme for methylmalonyl-CoA mutase) and methyl-Cbl (coenzyme for methionine synthetase) [6]. Haptocorrin also withdraws occasional Cbl-analogues from plasma circulation, preventing their incorporation into tissue where they may inhibit B_{12}-enzymes [7].

All of the currently known reactions of B_{12}-dependent enzymes involve the making and breaking of the Co–C bond [8,9]. AdoCbl is the cofactor in eliminase and mutase enzymes, which catalyze the intramolecular 1,2-shift of a hydrogen and an electronegative X group. An example is methylmalonyl-coenzyme-A mutase, which isomerizes reversibly the methylmalonyl group to a succinyl group. The rearrangement proceeds through a stepwise process initiated by the *homolytic cleavage* of the Co–C bond, with formation of two radicals, cob(II)alamin (B_{12r}) and adenosyl [9]. The former is a relatively long-lived species, while the latter rapidly abstracts a H atom from the substrate and then rearranges to the product, restoring the Co–C bond. AdoCbl has also been found to be the cofactor of the ribonucleotide reductase, which catalyses the conversion of nucleoside di- and tri-phosphates to deoxy analogues in some bacteria [10].

MeCbl-based enzymes (methyltransferases) catalyze the transfer of methyl groups from an N atom, as that in *N*-methyltetrahydrofolate (Me-FH_4), to cob(I)alamin (to form MeCbl) for onward transmission to an S atom of homocysteine to form methionine, as in methionine synthase. The overall mechanistic scheme requires a series of nucleophilic displacement reactions from cob(I)alamin to MeCo(III)Cbl species and vice versa [11]. MeCbl also plays a role in the pathway of carbon dioxide fixation in several anaerobic aceto-bacteria, as well as in the reversible pathway that results in formation of methane from acetic acid [12].

The X-ray structures of the AdoCbl and MeCbl free cofactors were reported for the first time in 1961 [13] and 1985 [14], respectively. Before 1994, due to the lack of structural information on coenzyme–enzyme binding, most hypotheses concerning such enzymatic mechanisms, particularly for homolysis, were based essentially on a wide-ranging study of simple models [15]. Model studies have furnished several insights into the factors which could play a role in the enormous enhancement of about 12 orders of magnitude of the homolysis rate for the holoenzyme with respect to the free coenzyme. The first X-ray crystal structure of AdoCbl-dependent methylmalonyl-CoA mutase [16] and ESR spectroscopy measurements [17] initially seemed to have launched a new era in coenzyme B_{12} bioinorganic chemistry. Specifically, the structure of the enzyme indicates that the coenzyme is present in its base-off form (Fig. 3), i.e. the appended 5,6-dimethylbenzimidazole nucleotide *is not bound to Co* (base-on form), *which is instead coordinated to the corrin α face to the imidazole of a histidine residue of the protein chain* (base-off/his-on). It appeared that this result could explain the enormous rate enhancement in the holoenzyme. Therefore, it seemed that not only was the axial Co–C bond, but also the axial Co–N bond, involved in enhancement of the homolysis rate as suggested by studies on simple models [18]. The histidine coordination to Co was also found in the structure of the MeCbl bound domain of methionine synthase [19]. However, more recent structural results have shown that the benzimidazole residue is still coordinated to Co in dioldehydratase, the coenzyme being in the base-on form (Fig. 3) [20].

Since then, the molecular structures of several B_{12}-enzymes have been reported [21]. But these do not have furnished further insight into the Co–C bond cleavage in AdoCbl-dependent enzymes. In fact, these results show that in mutases and aminomutases, AdoCbl binds the protein in the base-off/his-on mode [22], while in the eliminases and AdoCbl-dependent ribonucleotide reductase it binds the protein in the base-on mode [23].

Whereas the X-ray structures of several B_{12}-enzymes are available, no structural information on B_{12}-transporting proteins has so far been reported. Recently, the cloning of the cDNA encoding human and bovine transcobalamin has provided sufficient quantities of this Cbl-binding protein in pure form for X-ray structure determination [24]. Preliminary crystallographic results obtained in this laboratory have clearly shown that Cbl binds to the TC protein in the base-on form, but Co is coordinated *trans* to benzimidazole by a histidine residue of the protein, which has displaced a ligand, possibly a water molecule, from the β face [25]. Therefore, breaking and forming the Co axial bonds should also be involved in the binding of cobalamins to TC transporting proteins.

In addition to the above-discussed exciting aspects, cobalamins possess a number of functional groups found in biomolecules and crystallize with a large number of water molecules. In fact, the corrin ring bears several amido and a

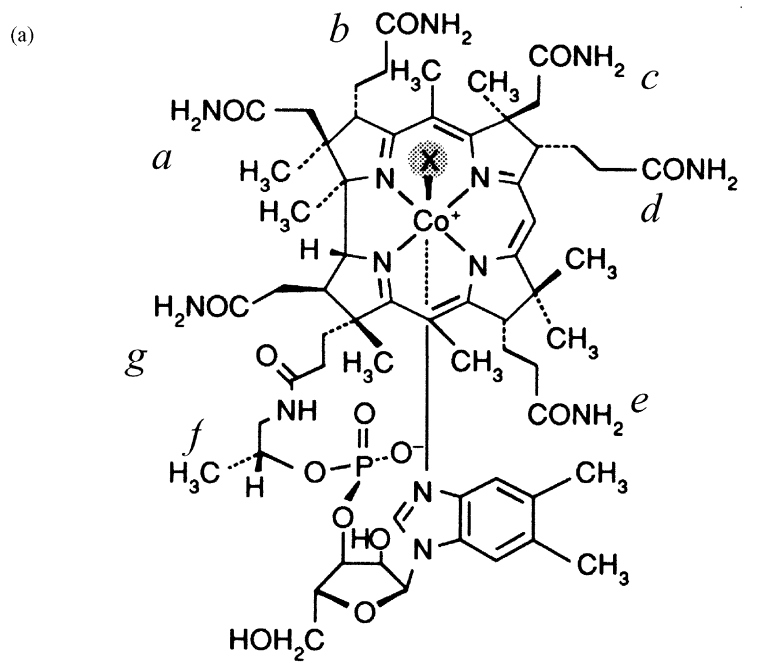

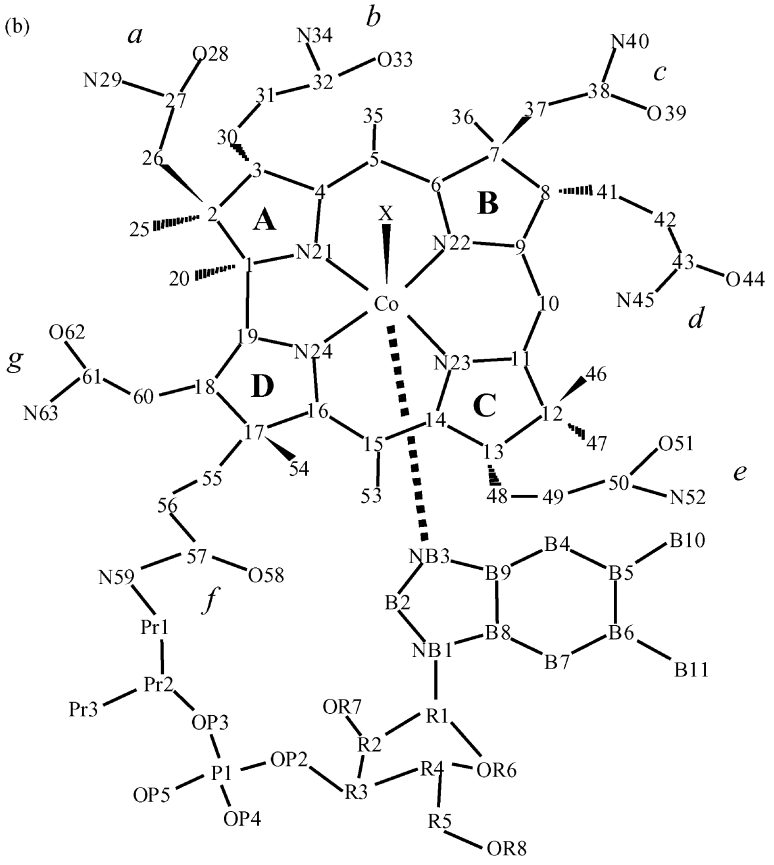

Fig. 1. (a) Structural formulas of Vitamin B_{12} and the most biologically relevant cobalamins. (b) Atom numbering scheme for Vitamin B_{12} and analogous cobalamins.

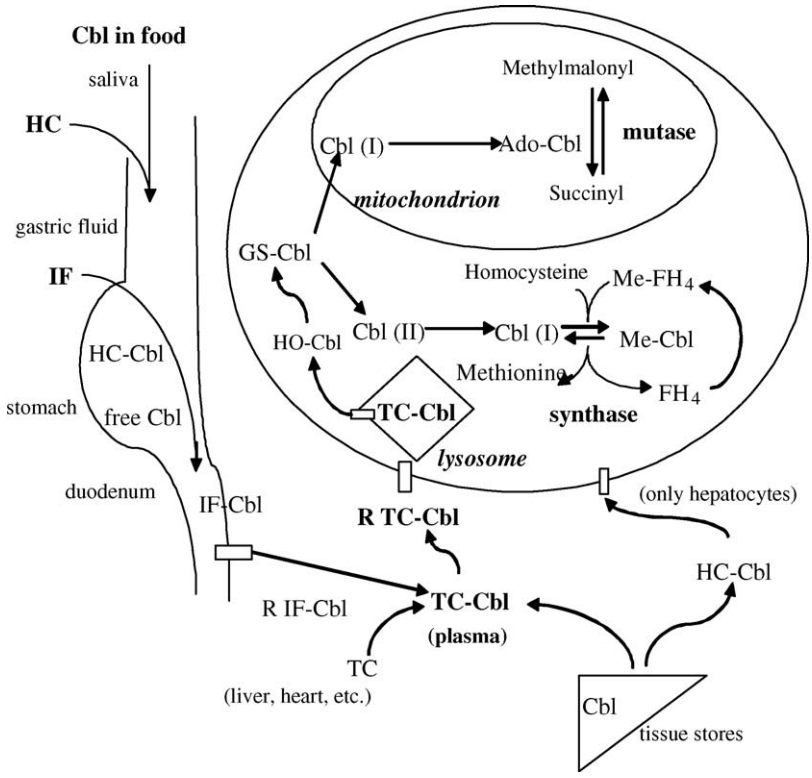

Fig. 2. Absorption, cellular uptake and enzymatic processes involving cobalamins in mammalians.

nucleotide chain (Fig. 1) and in the crystals there can be up to 20 molecules of water per cobalt atom. Therefore, cobalamins have been suggested as a particularly useful model for studying the interaction of water with proteins and nucleic acids, since they present a sizeable interface to the solvent, which makes them suitable to study the order–disorder arrangement in the water network in the presence of biomolecules [26].

Another important aspect has emerged from several studies which have shown that Vitamin B_{12} plays an important role [27] in the dechlorination of perchloro- (PCE) and trichloroethylene (TCE), which are widespread contaminants of soils and aquifers [28]. Several anaerobic organisms use corrinoid dependent enzymes to reductively dechlorinate these toxic compounds [29]. Vitamin B_{12} has been used in the catalytically abiotic dechlorination in the presence of strong reductants [30] and recent studies indicate that, also in this case, the breaking and forming of the Co–C bond is involved in this process [31,32].

Literature on structures of cobalamins is covered up to 1999 by two reviews [33,34]. More recently, some additional NMR and X-ray structures of organocobalamins have been reported in the extensive review by Brown on chemistry and enzymology of Vitamin B_{12} [21a].

In the present review, we discuss the crystal chemistry of cobalamins, the geometry of the corrin ring and of the X–Co–NB3 axial fragment. The latter aspect will be discussed in comparison with that of its well-known model molecules, the cobaloximes (Scheme 1) [15].

No reference to the considerable amount of theoretical calculations, both by DFT [21a] and MM-MD [21a,35] techniques, is given since they have been recently reviewed.

2. Crystal chemistry

The main crystallographic features of cobalamins in the solid state are described in this section. Particularly, it is shown that the crystal packing of these large molecules is primarily determined by intra- and intermolecular H-bond interactions.

2.1. Crystal packing in cobalamins

It has been shown [33,36] that the vast majority of cobalamins which crystallize in the $P2_12_12_1$ space group, are isomorphous and can be assigned to four groups (clusters) **I**–**IV**, characterized by different values of the cell axis ratios *c*/*a* and *b*/*a* (Fig. 4). MeCbl and $(H_2OCbl)^+$ cannot be assigned to any of these clusters [36].

The large cobalamin molecules have a roughly spherical shape and, as first observed by Hodgkin et al. [37], their crystals can be considered as built up by stacking of distorted close-packed layers of XCbl molecules. A typical distorted close-packed layer is sketched in Fig. 5, which shows that each molecule is surrounded by six others in a roughly hexagonal arrangement. Crystal packing analysis shows that each cluster corresponds to a different stacking of the same distorted close-packed layers of the cobalamin molecules [33,36]. If we consider the Co atoms as the centres of the spheres, a typical stacking of the layers, whose mean planes are separated by one half of the *c* edge of the unit cell, is sketched in Fig. 6a. This stacking resembles the well-known hexagonal close packing (hcp) of spheres shown in Fig. 6b, where each sphere is in contact with 12 others, six in the plane, three below the plane and three above the plane.

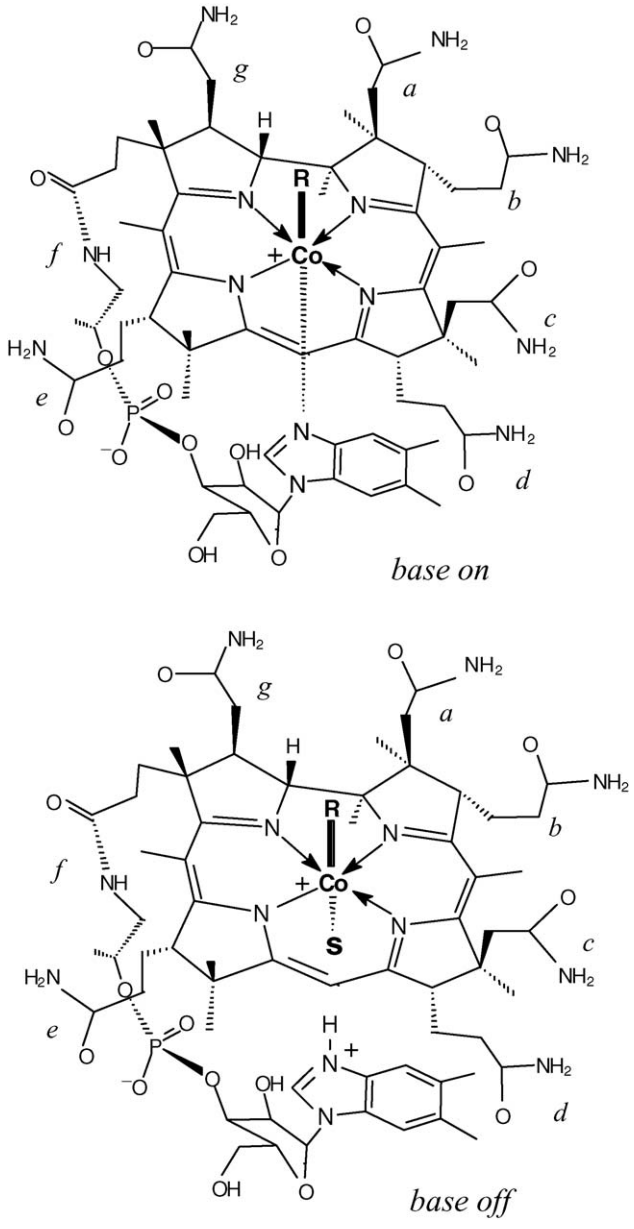

Fig. 3. The base-on and base-off form of a cobalamin.

The corresponding 12-fold environment about each sphere in the packing of cobalamin is significantly distorted with respect to the truncated cuboctahedron of the hcp packing. In fact, while all the centres of the spheres in each stacked plane are coplanar

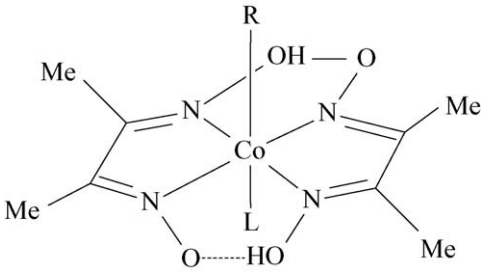

Scheme 1.

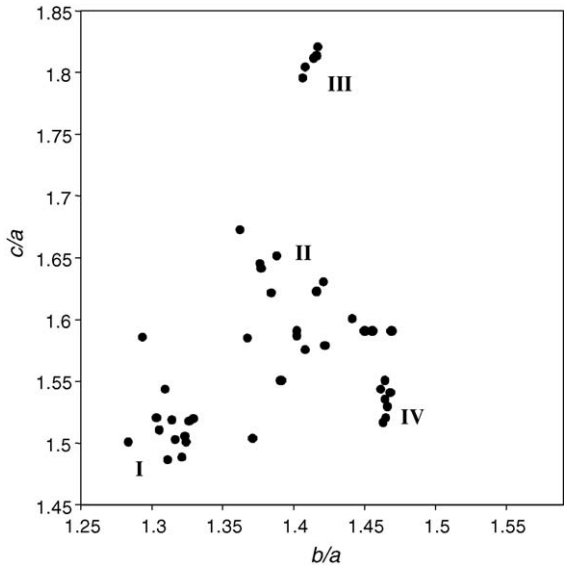

Fig. 4. Scatter plot of unit cell ratio *c/a* vs. *b/a* for cobalamins grouped in the four clusters **I**–**IV**.

in the hcp arrangement, this is not the case for the Co centres of each stacked plane of Fig. 6a. Therefore, each plane is corrugated with a "depth", measured by the difference, Δz, between the Co centres above and below the plane, as represented by different types of circles in Fig. 6a. Furthermore, the shift between the adjacent layers, measured by the vector **S**, is shorter than that in the hcp packing. The packing in the four clusters differs in **S** and Δz [38].

The layers are packed in such a way as to form large cavities filled by the solvent molecules, generally water molecules [26], or ions [39]. The ligand X is also located in the channel, irrespective of the ligand shape. The cavities can be described as being comprised of a central channel running along the crystallographic screw axis and connected to side pockets at intervals defined by this screw axis (Fig. 7). The crystal structure has been investigated in depth in the case of AdoCbl by neutron diffraction analysis [26]. The shapes of the cavities in clusters **I**, **II** and **IV** are similar, but differ somewhat from that accurately analyzed in AdoCbl [26] (see next section).

2.2. H-bond network

An ordered H-bond network of water molecules with full occupancy characterizes the pocket region of the cavity, whereas the channel is occupied by a disordered pattern of water molecules, generally having fractional occupancy, as found in AdoCbl [26b]. The only exception to this ordered–disordered scheme of solvent within the cavity was found in $NH_4[(SO_3)Cbl]$ [40], which crystallizes with one glycerol molecule per Co atom. In fact, it is the presence of the glycerol within the channel which allows an ordered H-bonding pattern of the water molecules (Fig. 7). On the other hand, attempts to solve the structure of glutathionylcobalamin (GSCbl, GS = γ-glutamylcysteinylglycine) were hampered by the severe disorder of the GS moiety in the channel, with only the first atoms of the GS ligand located [41].

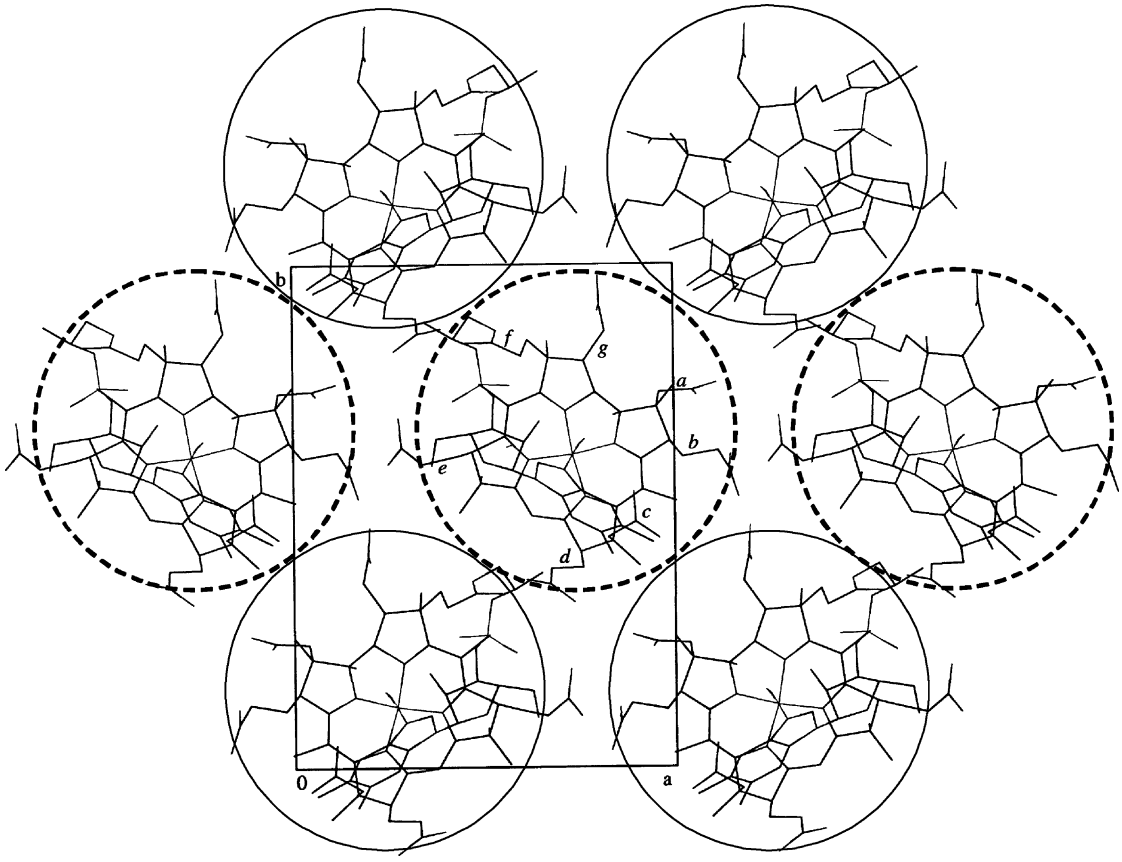

Fig. 5. A typical distorted close-packed layer of cobalamins. The roughly spherical cobalamin molecules above and below the layer mean plane, are represented by full and broken circumferences, respectively.

Five ordered water molecules (Ow1–Ow5) within the pocket are conserved in many cobalamin structures, with either three or four H-bond coordination. If alkali metal or ammonium ions are present in the crystal, the water molecule Ow5, which has a four oxygen environment, is replaced by a positive ion as shown in Fig. 7, in the case NH_4^+.

The solvent structure in the channel has been determined by means of high resolution neutron diffraction at 15 K, which allowed identification of the disordered water peaks in the channel of the AdoCbl crystals and formulation of two main solvent networks per asymmetric unit [26b]. Both networks are composed of 17 water molecules, with H-bond coordination ranging from two to five. Furthermore, analysis of the water arrangement around apolar groups of AdoCbl indicated the presence of clathrate-like water structures. This result confirmed the structural principles that control water geometries in hydrating biomolecules [26b].

It has been shown that cobalamins belonging to the same cluster have very similar conformations for all the amide side chains (see next section) and very similar intra- and intermolecular H-bond patterns [42]. In particular, cobalamins belonging to clusters **I** and **IV** are characterized by a *c* chain conformation such that the amide group is directed towards the X axial ligand, forming an intramolecular H-bond with the latter. In addition, the conformations of the *e* and *f* chains in cobalamins of groups **IV** are arranged in such a way as to form another intramolecular H-bond between OR8 (chain *f*) and O51 (chain *e*). Cobalamins of groups **II** and **III** do not form intramolecular H-bonds and their amide side chains are involved in intermolecular H-bonding with each other and with water molecules [42]. A few exceptions however occur, as in the recently determined X-ray structure of NO_2Cbl·NaCl [38], which is characterized by an intramolecular H-bond between the *c* amide chain and the axial nitro group, even if it belongs to cluster **II**.

These observations suggest that the observed differences between cobalamin packing are determined, to a large extent, by the different involvement of the amide side chains in intra- and intermolecular H-bonds. In fact, all the cobalamins belonging to clusters **I** and **IV** have an axial ligand suitable to form H-bonds with the *c* amide chain.

2.3. Ionic species in cobalamins co-crystallized with electrolytes

A series of results [43] suggested the existence of weak bonding interactions between cobalamins and charged species, which influence their behaviour in solution. The interest in the study of these interactions resides in the possible role that they could play in determining the organo-group transfer reaction of B_{12}-enzymes. A structural picture, at least in the solid state, of the interactions between cobalamins, water molecules and charged species was obtained by the crystal structure analysis of cobalamins crystallized in the presence of highly concentrated alkali metal chloride salts. Several inorganic cobalamins of formula

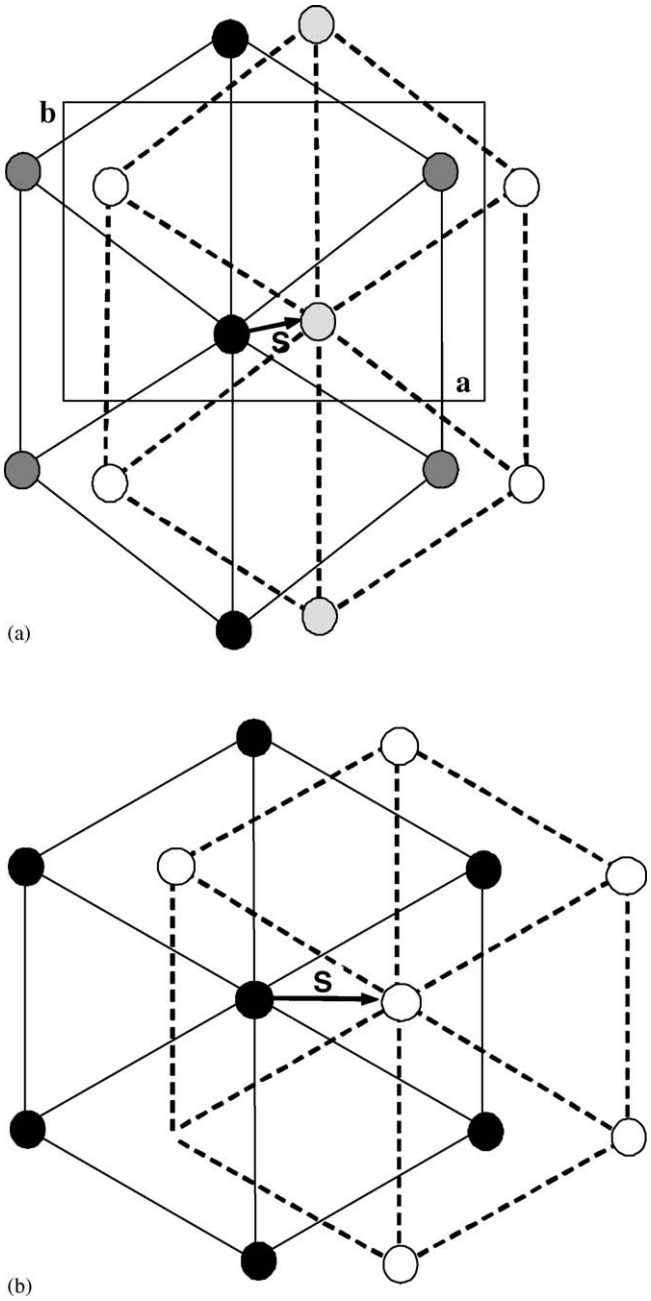

Fig. 6. Sketch of (a) the stacking of the distorted close-packed planes in cobalamin crystals and (b) the ideal hexagonal close packing. **S** is the vector measuring the minimum distance between two cobalt atoms belonging to two adjacent planes.

XCbl·2LiCl (A) and XCbl·Na(K)Cl (B) were crystallized and structurally characterized [38,39,42].

The typical arrangement of ions in species of formula A is depicted in Fig. 8, showing that all the amide side chains except chain *c* which is involved in the intramolecular H-bond, interact with Cl^- and Li^+ ions. In addition to water molecules, the nearly tetrahedral cations are coordinated to three amidic O atoms and to OP4 of the phosphate group, whereas the anions are held by NH···Cl hydrogen bonds to amidic N atoms of the chains and to water molecules. Cl1 has a distorted trigonal arrangement of amidic N atoms, whereas Cl2 has a distorted environment of two water molecules and one amidic N atom. One pair of Cl^- and Li^+ ions makes a short contact of 4.079(5) Å. Each cobalamin is surrounded by eight ions, three of which (one Li^+ and two Cl^-) lie above the β face and five (four Li^+ and one Cl^-) above the α face. This suggests that the β face is more negatively charged [39].

The arrangement of ions in species of formula B is depicted in Fig. 9. Each K^+ ion is coordinated by O39 and O62 of two different cobalamin molecules and by OR8 and OP4 of the *f* chain of one of the two molecules, in a distorted pyramidal arrangement with OP4 at the apex. The Cl^- ion receives four H-bonds from N34, N59, OR8 and a water molecule. The anion and cation, bridged by OR8, make a short contact of 3.086(5) Å.

3. The equatorial moiety

The equatorial moiety of cobalamins consists of the chiral ligand, called corrin. The corrin has a single helical sense (left-handed) of absolute *R* configuration of its chiral centres at C1 and C19 (Fig. 1b). The atom numbering scheme, introduced by Hodgkin [44] and Glusker [45], is commonly used. When viewed from the β (upper) face, on the axial X ligand side, the atoms of the corrin ligand are numbered in a clockwise sense from C1 to C19 and the methyl group bonded at C1 is on the α (lower) face (Fig. 1b). The four pyrrole rings are indicated clockwise as A–D. The seven amide side chains are labeled as *a–g* in the same sense and their atoms are numbered accordingly. Their orientation at the corrin periphery is described as α or β for chains directed on the lower or the upper half space of the corrin, respectively. The three acetamide groups (*a*, *c*, *g*) protrude above the corrin, and the four propionamide groups (*b*, *d*, *e*, *f*) below. A side view of a cobalamin, stressing (in black) the bond of the first atom of the corrin side chains *a–d* and of the corrin side methyl groups, is shown in Fig. 10. These atoms, called *sentinel* [45], control the access of the axial ligands to the Co centre and their orientation with respect to the equatorial moiety.

3.1. Bond lengths in the corrin ring

The mean values of bond lengths of the corrin nucleus were reported many years ago [45]. However, these values were based on the limited number of structure determinations of low accuracy at that time available. More recently, thanks to the availability of numerous accurate structure determinations, most based on synchrotron data, a more accurate analysis of the bond lengths within the corrin moiety has been performed and the results rationalized in terms of electronic and steric factors [42]. Thirteen structure determinations with $R \leq 0.08$ were considered and the corresponding values of those distances within the corrin nucleus were averaged. The mean values, together with their standard deviations, are given in Fig. 11. The very low values of the estimated standard deviations of the mean, strongly suggest that the bond lengths of the equatorial moiety are scarcely affected by the kind of the axial ligand X.

First of all, the Co–N equatorial distances involved in the five membered ring are shorter than the other two equatorial

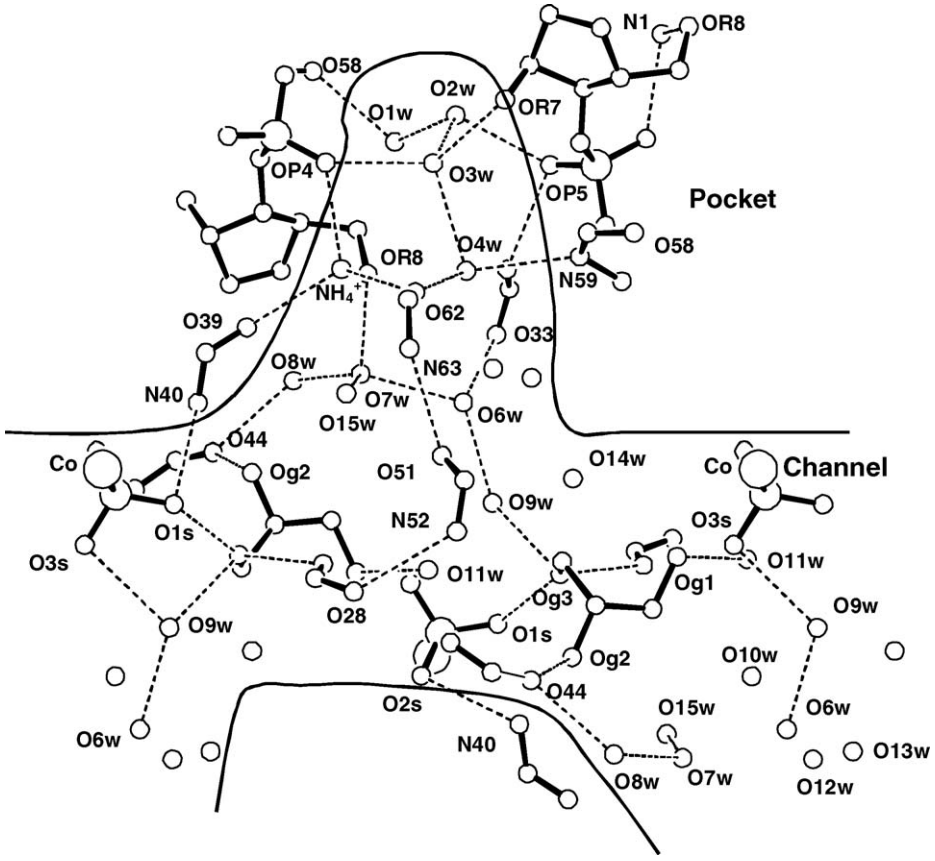

Fig. 7. H-bonding scheme (dashed lines) within the pocket and the channel in $(SO_3Cbl)(NH_4)$.

Co–N distances by about 0.020 Å. The distances of the delocalized inner portion of the corrin ligand, from N21 to N24 clockwise, are those expected for a conjugated system of C–C and C–N bonds, and their trend reflects an approximately two-fold symmetry with respect to the axis passing through Co and C10 (Fig. 1). The trend can be qualitatively interpreted on the basis of the four resonance structures, sketched in Fig. 12.

Recent ab initio calculations, the only ones carried out on Ado-, Me-, CN- and OHCbl molecules with all the atoms of Fig. 1 (all the other DFT calculations have been so far carried out on the so called "corrin model" [21a], an exemplified corrin moiety where H atoms substitute all the corrin side chains and methyls) gave bond order values in agreement with the experimental bond lengths [46,47]. These calculations also allowed

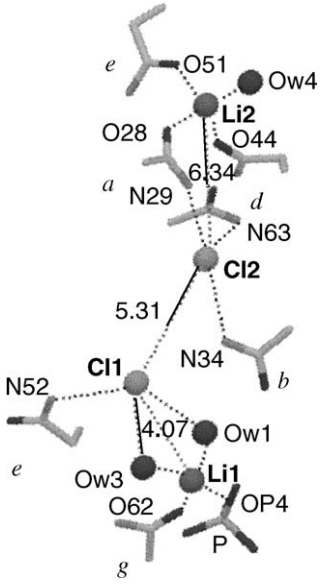

Fig. 8. Scheme of H-bonds involving anions and of cation coordination in crystals of cobalamins with composition XCbl·2LiCl. Interionic distances are given in Å.

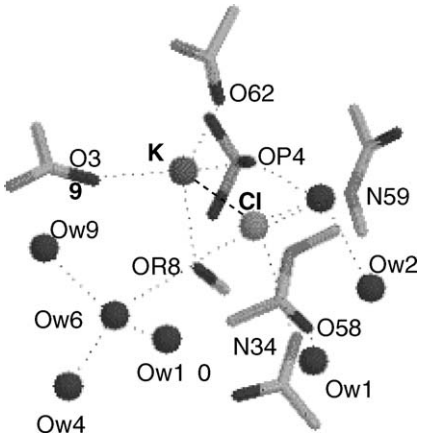

Fig. 9. Scheme of H-bonds involving anions and of cation coordination in crystals of cobalamins with composition XCbl·KCl.

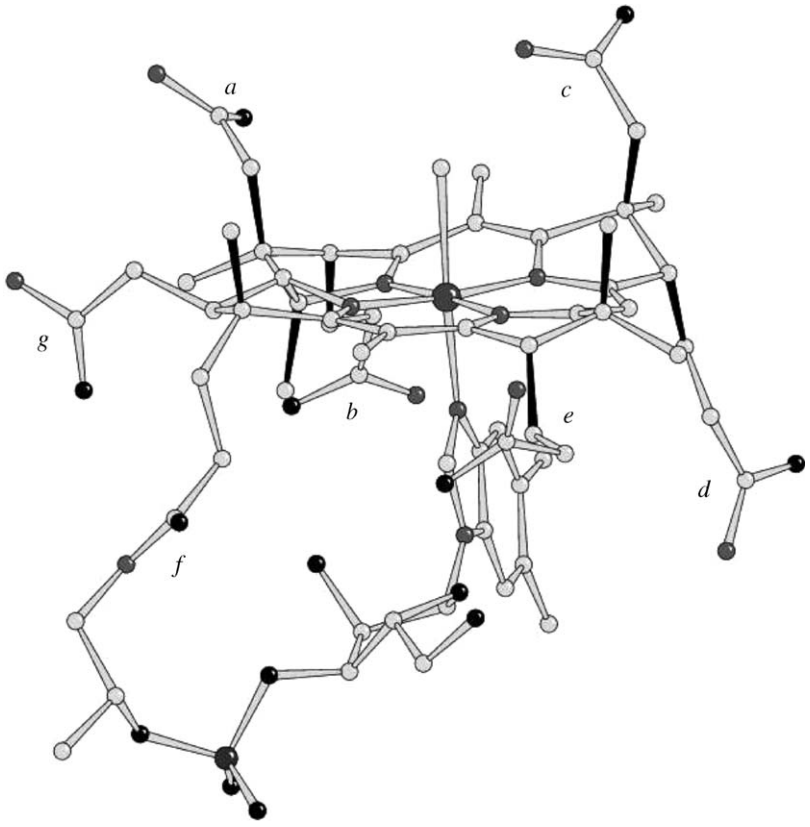

Fig. 10. Side view of ClCbl evidencing the "sentinel" atoms which form bonds to the corrin (black sticks).

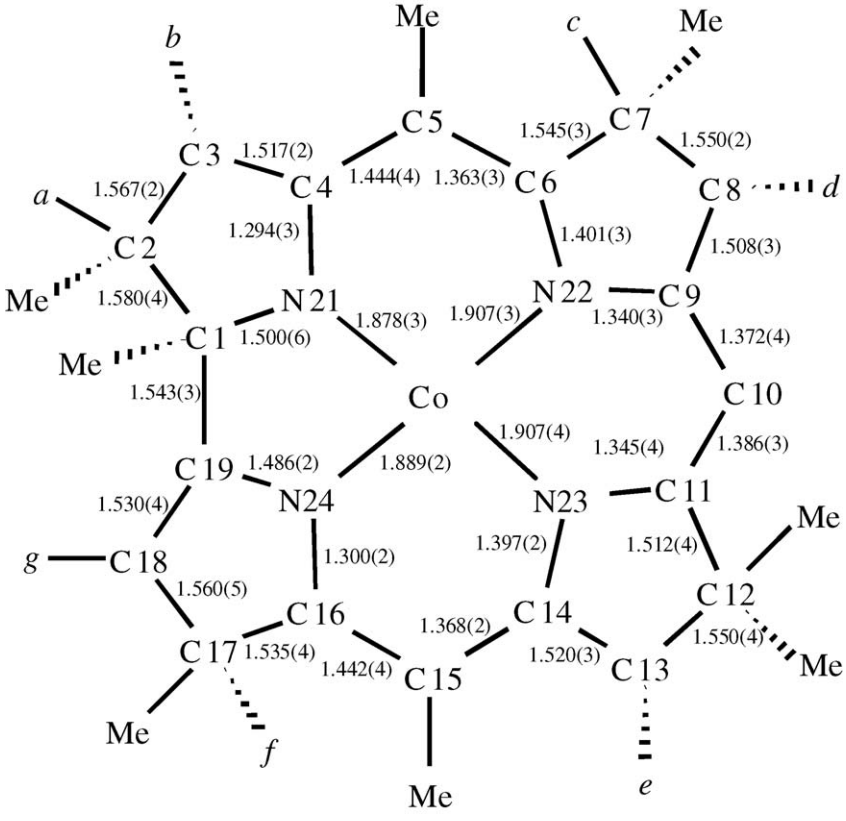

Fig. 11. Mean bond lengths within the corrin nucleus. Numbers in parentheses represent the standard deviation of the mean, $\sigma = [\sum(x - x_m)^2/(n(n-1))]^{1/2}$.

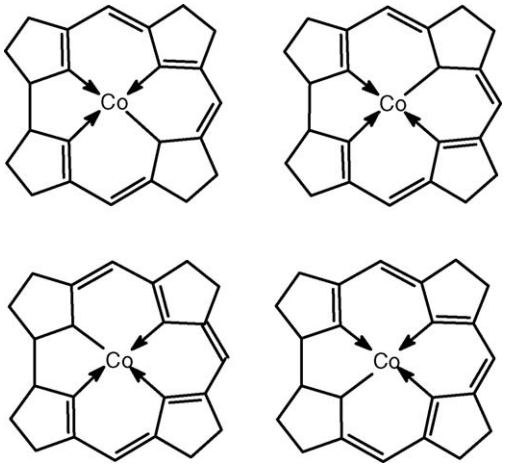

Fig. 12. The main four resonance structures for the delocalized corrin moiety.

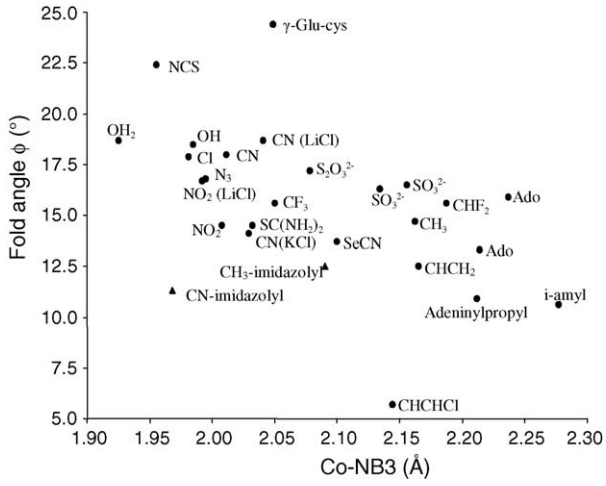

Fig. 13. Scatter plot of the corrin fold angle ϕ (see text) against the axial Co–NB3 distance. Triangles refer to the imidazolyl analogues.

interpretation of the X-ray emission and X-ray photoelectron spectra of CNCbl and MeCbl [46b].

The trend of the C–C single bond lengths of the external portion of the corrin, which vary from 1.508 Å (C8–C9) to 1.580 Å (C1–C2), reflects the different hybridization of the bonded C atoms as well as the number of their non-H substituents. Accordingly, the mean values of the chemically equivalent bond lengths vary in the order:

$$\underset{(1.580\,\text{Å})}{C_q\text{–}C_q} > \underset{(1.555\,\text{Å})}{C_q\text{–}C_t} > \underset{(1.532\,\text{Å})}{C_t\text{–}C_t} \approx \underset{(1.532\,\text{Å})}{C_q\text{–}C(sp^2)} > \underset{(1.513\,\text{Å})}{C_t\text{–}C(sp^2)}$$

where C_q and C_t represent quaternary and tertiary C atoms, respectively. The corresponding mean values are given in parentheses. The long C_q–C_q bond reflects the overcrowding of the side groups of the corrin five-membered ring (Fig. 1).

3.2. The folding of the corrin ligand

The preferred mode of deformation of the corrin ligand is represented by a folding towards the X axial ligand, about an axis approximately bisecting the C1–C19 bond and passing through C10. The deformation is measured by the folding angle ϕ, which is generally calculated as the dihedral angle between the planes passing through N21, C4, C5, C6, N22, C9, C10 and C10, C11, N23, C14, C15, C16, N24 (Fig. 1b). The folding angle ϕ of the corrin moiety was originally suggested [45] to reflect the bulk of the axial X ligand, decreasing as the latter increases. However, more recently it has been observed [33] that ϕ decreases with increasing Co–NB3 distance, i.e. with an increase in the *trans* influencing ability of X, rather than with its bulk. An increase of about 0.4 Å corresponds to a decrease of about 15° in ϕ (Table 1), which has been attributed to the release of the steric pressure of the benzimidazole residue on the equatorial ligand, due to the lengthening of the Co–NB3 bond induced by the increase in the *trans* influencing ability of X. The fact that Co-β-cyano-imidazolylcobamide [48] and Co-β-methyl-imidazolylcobamide [49] (i.e. CNCbl and MeCbl analogues having the imidazole instead of the benzimidazole residue in the *f* chain) do not fit the trend ($\phi = 11.3(2)°$ and Co–B3 = 1.968(9) Å in the cyano derivative and $\phi = 12.5°$ and Co–NB3 = 2.09 Å in the methyl derivative) was attributed to the smaller bulk of the imidazole with respect to the benzimidazole residue [33]. ϕ Values for several cobalamins determined with high accuracy are given in Table 1, together with the Co–NB3 distances having E.S.D.'s ≤ 0.01 Å.

The data appear to confirm the previously observed trend of ϕ against the Co–NB3 distance, given in Fig. 13, where the very recent structure of *i*-amylCbl [50], which has the smallest value of the folding angle (10.6°) and the longest Co–NB3 distance (2.277(2) Å) so far reported, is even below the imidazolylcobamide points. However, γ-glutamylcysteinylcobalamin ((γ-glu-cys)Cbl), the first thiolatocobalamin structurally characterized [51] is out of the trend of Fig. 13, having the largest fold angle so far reported in a cobalamin. Analogously, CNCbl·KCl compared to CNCbl(LiCl) also does not follow the trend, the relative point being significantly shifted towards the imidazolyl side. This suggests that additional factors, such as the packing, could influence the fold angle, although to a limited extent. It may be concluded that the *endogenous* wave deformation of the corrin moiety, due to the saturated over crowded five-membered cycle, is further affected by the *exogenous* electronic *trans*-influence of the axial X ligand, which modulates the steric pressure of the benzimidazole moiety.

3.3. Conformation of the amide side chains

As shown in Fig. 10, the acetamide side chains *a* and *c* lie axially above the corrin ring (on the β face) and the propionamide side chains *b*, *d* and *e* lie axially below. The acetamide chain *g* is equatorial, as is chain *f*. The earlier analysis, carried out by Glusker [45] on the basis of the X-ray cobalamin structures available at that time, including mono and hexa carboxylic acids and yellow corrinoids, suggested that the conformation of *a* and *b* side chains in particular, but also of *f* and *g* chains, was essentially constant, whereas the other chains exhibit variability, particularly the chain *e*. The side chains with the most conformational variability appeared to be on rings B and C (Fig. 1b).

Table 1
Bond lengths to axial Co ligands for cobalamins and cobaloximes with E.S.D.'s ≤ 0.01 Å

X	XCbl				$XCo(DH)_2py$[a]	
	Co–X (Å)	Co–NB3 (Å)	Fold angle (°)	Reference	Co–X (Å)	Co–N(py) (Å)
OH_2	1.952(2)	1.925(2)	18.7	[52]	1.916(3)	1.926(3)
NCS	1.955(11)	1.955(9)	22.4	[70]		
Cl	2.252(1)	1.981(3)	17.9	[39]	2.229(1)	1.959(2)
OH	1.920(4)	1.985(5)	18.5	[17]		
NO_2 (LiCl)	1.942(6)	1.992(6)	16.7	[38]	1.943(3)	1.985(2)
NO_2	1.941(5)	2.008(4)	14.5	[70]		
NO_2 (NaCl)	1.93(1)	2.014(5)		[38]		
N_3	1.980(3)	1.995(3)	16.8	[39]	1.950(3)	1.973(1)
CN	1.858(10)	2.011(10)	18.0	[48]	1.937(2)	1.995(2)
CN(KCl)	1.868(8)	2.029(6)	14.1	[42]		
CN(LiCl)	1.885(4)	2.041(3)	18.7	[42]		
$SC(NH_2)_2$	2.300(2)	2.032(5)	14.5	[40]		
γ-Glu-cys	2.267(2)	2.049(6)	24.4	[51]		
CF_3[b]	1.88(1)	2.05(1)	15.6		1.949(4)	2.043(3)
$S_2O_3^{2-}$	2.286(1)	2.078(3)	17.2	[70]		
SeCN	2.394(2)	2.100(7)	13.7	[70]		
	2.384(3)	2.020(5)		[38]		
CHCHCl	1.951(7)	2.144(5)	5.7	[31]	1.947(2)[c]	2.046(2)[c]
SO_3^{2-}	2.231(1)	2.134(4)	16.3	[36]	2.225(2)[d]	2.042[d]
	2.241(2)	2.156(5)	16.5	[40]		
CH_3	1.979(4)	2.162(4)	14.7	[42]	1.998(5)	2.068(3)
$CH{=}CH_2$	1.911(7)	2.165(6)	12.5	[31]	1.953(3)	2.052(2)
CHF_2	1.949(8)	2.187(7)	15.6	[64]	1.948[d]	2.040[d]
$PO(iPrO)_2$[e]	2.227(1)	2.189(2)				
Adeninylpropyl[f]	1.959(10)	2.212(8)	10.9			
Ado	2.033(4)	2.237(3)	15.9	[26]	2.015(2)	2.072(2)
Ado	2.023(10)	2.214(9)	13.3	[46]		
i-Amyl	2.044(3)	2.277(2)	10.6	[50]		

[a] Data for cobaloximes are given in Refs. [15,42] if not otherwise stated.
[b] Ref. [84].
[c] Ref. [85].
[d] Calculated values.
[e] Ref. [86].
[f] Ref. [87].

More recently [42], a more extensive analysis of the chain conformation was carried out on many cobalamins whose accurate X-ray structures became available in the last 20 years. First of all, this analysis has shown that the conformations of the amide side chains are similar for cobalamins belonging to the same cluster. The superposition of several cobalamins, belonging to the same cluster, is reported for each cluster in Fig. 14, taking into account that in the case of cluster **III** the X-ray and neutron structures are superimposed. In each cluster, the conformations of the side chains are very similar if the amide group orientation, which covers a wide range of positions, is excluded.

Inspection of Fig. 14 indicates that side chains *a* and *d* assume very similar conformations in all the clusters, chain *g* essentially two conformations, while the others have a larger conformational freedom [42]. It should be mentioned, however, that exceptions occur. For example, the conformation of the *c* chain in OHCbl, which belongs to cluster **I**, does not superimpose well with the others of its cluster, but is very close to that of aquacobalamin. This is easily explained by the similarity of the H-bond formation between the *c* chain and the axial ligand in the two cases (see below). In addition, the superposition of $ClCbl{\cdot}(LiCl)_2$ (cluster **IV**) and H_2OCbl^+ (Fig. 15) structures shows that the conformation of the side chains are similar, although the latter does not belong to any cluster, on the basis of the unit cell ratios.

It is worth noting that comparison of the H-bond scheme involving the β axial ligand and the *c* chain in OHCbl and H_2OCbl^+ shows that a conserved crystallization water molecule receives [52] and donates a H-bond to the axial O atom, respectively (Fig. 16), with concomitant change of the H-bond distance to the O of the *c* chain and variation of the geometry of the axial fragment. This structural change corresponds to a log *K* of 6.2 [53] for the reaction:

$$H_2OCbl^+ + OH^- \rightleftarrows OHCbl + H_2O$$

It should be noted that in AdoCbl [26,47] (Fig. 14), as well as in MeCbl [42], the amido group plane of the *d* chain is approximately perpendicular to the benzimidazole plane, so that one of its H atoms points towards the centre of the benzene ring. Theoretical calculations have suggested that such an interaction results in an energy stabilization of 16.7 kcal/mol [54].

The solution structure of MeCbl, determined by NMR spectroscopy, has been reported [55]. In solution, the *a* and *d* chains were found to have a notable conformational rigidity, whereas

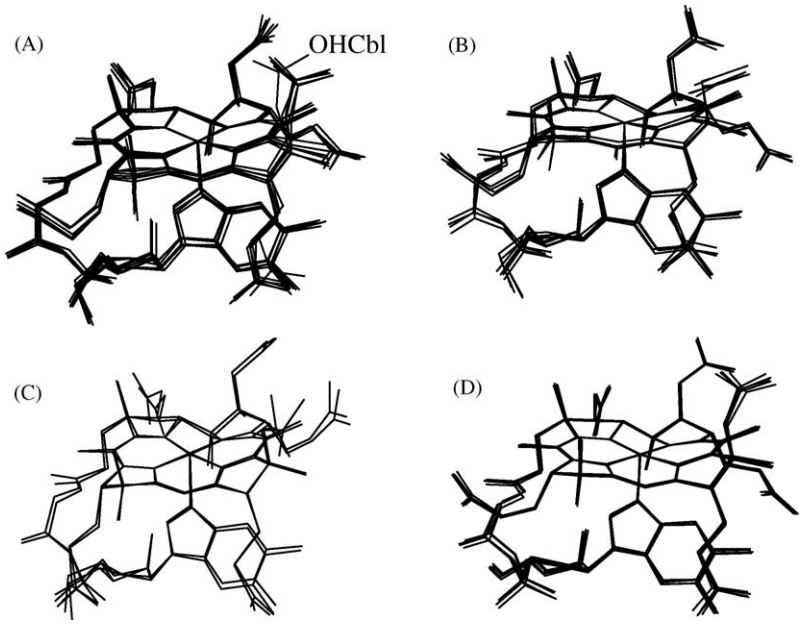

Fig. 14. Superposition of some cobalamin skeletons for (A) cluster **I** (CN-Cbl·KCl, $(NH_2)_2$CS-Cbl, OH-Cbl, (*R*)-2,3-dihydroxypropyl-Cbl, (*S*)-2,3-dihydroxypropyl-Cbl, CN-Cbl (dry)), (B) cluster **II** (CN-Cbl (wet), NCSe-Cbl, O_2-Cbl, CN-Cbl (acet.)), (C) cluster **III** (Ado-Cbl (15 K), Ado-Cbl (295 K)) and (D) cluster **IV** (Cl-Cbl·2LiCl, N_3-Cbl·2LiCl, NO_2-Cbl·2LiCl, CN-Cbl·2LiCl, Br-Cbl·2LiBr (all at 100 K)). The X axial group is omitted for sake of clarity.

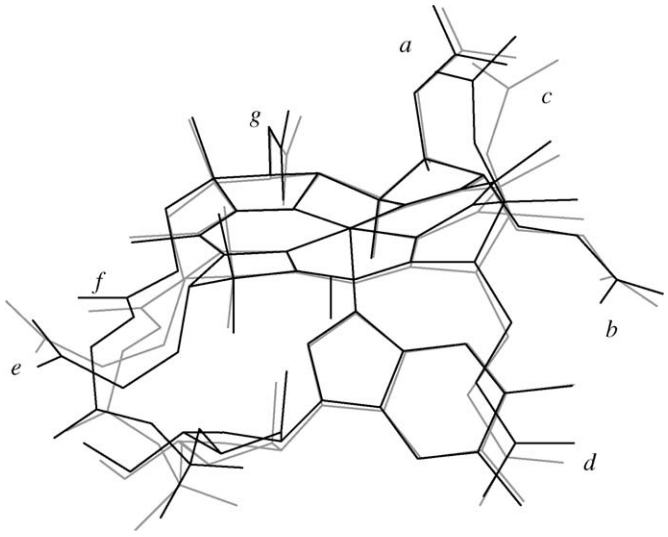

Fig. 15. Superposition of the skeleton of H_2OCbl^+ (black) with that of ClCbl·2LiCl (gray).

the *b*, *c*, *e* and *g* chains were flexible to different extents. This result corresponds nicely to that derived from the above reported analysis of the chain conformation and it is also supported by the detailed description of the internal motions of MeCbl and CNCbl in solution by NMR-restrained modeling [56]. However, the comparison with the low accuracy X-ray structure of MeCbl underlined several conformational differences within the nucleotide loop [55]. The new, more accurate structural redetermination of MeCbl [42] has shown that the solution and the solid state conformations of the nucleotide loop are much more similar than originally believed, despite the presence in the crystals of ionic species (LiCl).

The comparison of MeCbl in solution and in the solid state indicates that these biomolecules, highly hydrated in the solid state, should have a conformation similar to that in solution.

4. Structural properties of the cobalamin axial fragment

As has been stressed in Section 1, the binding of Me- and AdoCbl to their apoenzymes of B_{12} based methyltransferase and

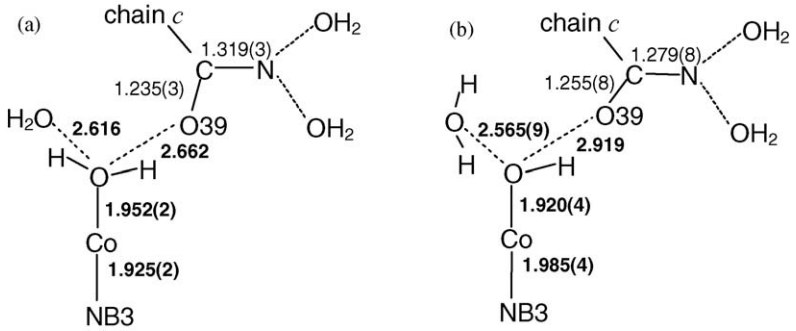

Fig. 16. Sketch of the H-bond pattern involving the axial β ligand and the corrin chain *c* in (a) H_2OCbl^+ and (b) OHCbl with relevant distances in Å.

mutases, respectively [1,2] as well as to the transporting protein TC [25], involves the breaking and forming of the axial bonds of the cobalamin. Furthermore, the enzymatic mechanisms are generally believed to involve breaking and making the Co–C bond. Therefore, the study of these processes requires the best possible knowledge of the nature and properties of the axial fragment in the isolated and protein bound cobalamins. From a structural point of view, the large number of accurate Cbl structures now available allows a quite good characterization of the axial fragment. The lower accuracy of enzyme structural data, at the present time, does not allow a similarly accurate characterization, and hence a meaningful comparison between protein bound and unbound cobalamins is not possible. Notwithstanding this, the discussed question (also complicated by confusing EXAFS conclusions [57]) about the length of the axial Co–N distance in the base-off/his-on protein bonded AdoCbl has been elegantly solved by Kratky and co-workers using EXAFS [58] and X-ray diffraction [59] experiments. These authors concluded that the Co–N axial bond in the enzymes should not be much longer than that in the isolated cobalamins.

The interactions between the β axial ligand and both the equatorial corrin and the α axial ligands, which could be exploited by the protein to control the reactivity, can be described in terms of *cis* and *trans* effects in these octahedral Co(III) complexes. These effects have been clearly outlined by Pratt [53] for an axial X–Co–Y fragment. They can be studied by examining: (a) the ground state effects, i.e. the effects of varying X on physical properties of the *trans* ligand Y, such as bond lengths and stretching constants; (b) thermodynamic effects on the equilibrium constants for ligand substitution reactions of the X/Y pair, which involve the difference in free energy between two ground states of potentially known structure; (c) kinetic effects for the reaction of type (b), which involve the difference in free energy between the ground state and the transition state. The last-mentioned effects are usually called *cis* and *trans* effects, whereas those on points (a) and (b) are usually called *cis* and *trans* influences.

We will principally concentrate on the structural properties of the axial fragment of the free cobalamins, whose Co–NB3 and Co–X distances, with estimated standard deviations ≤0.01 Å, are reported in Table 1.

4.1. The coordination of the benzimidazole residue in cobalamins

The plane containing the benzimidazole residue approximately bisects the two opposite six-membered rings of the corrin. This orientation, directed by the interaction with the corrin sentinel groups, is approximately the same in all the cobalamins (Fig. 10). In the base-on form, coordination of NB3 to Co is "asymmetric", that is, characterized by a large difference of about 10° between the two Co–NB3–C bond angles, because of the lopsided benzimidazole ligand. Typically, the Co–NB3–B2 and Co–NB3–B9 angles (Fig. 1b) are 122° and 132°, respectively, the larger angle being on the side of the benzimidazole phenyl ring. On the contrary, the axial N coordination in the imidazolyl cobinamide analogues [48,49] is "symmetric", the two Co–N–C angles being approximately equal and typically around 127°. The different angular coordination about the N axial donor corresponds to a Co–N distance in cobalamins which is longer by about 0.07 Å than that in imidazolylcobamides [48]. Although the values of bond lengths and angles in proteins must be carefully considered owing to their low accuracy, there is a clear indication that coordination to Co of the imidazole of the histidine residue in mutases is asymmetric, probably because of the strain imposed by the protein chain. Typical values of the Co–N–C angles are similar to those of 121° and 130° found by Reitzer et al. [59] in the glutamate mutase reconstituted with either CN and MeCbl, bound in the base-off/his-on mode, at a resolution of less than 2.0 Å. The corresponding Co–N distances are 2.28 Å in the cyano and 2.34 Å in the methyl cofactors, differing by about 0.06 Å. This difference should be compared to that of 0.11 Å found between the Me (2.09 Å) and the CN (1.968(9) Å) imidazolylcobamides [48,49]. However, these authors have correctly interpreted the values of 2.28 Å in the cyano and 2.34 Å in the methyl cofactors as the average of the very long distance (2.5 Å) of the pentacoordinated Co(II) species and the correspondingly shorter distance of the hexacoordinated Co(III) species. In fact, they have found that the protein crystals should contain the cofactor with 50% in hexacoordinated and 50% in pentacoordinated form. Hence, they concluded that "the protein bound B_{12} cofactor in the Co(II) state has an axial Co–N bond to the lower ligand that is not much longer (if at all) than that deduced from crystallography of cobalamins or cobamides" [59]. However, data available from cobaloximes and other simple B_{12} models indicate that the asymmetric coordination of 1,2-dimethylimidazole corresponds to a lengthening of the axial Co–N of about 0.06 Å with respect to the symmetric coordination of 1-methylimidazole, as found in the so called Costa model [15] (Scheme 2).

4.2. cis and trans effects in cobaloximes

Before analysing these effects in cobalamins, let us summarize the results of their analysis in cobaloximes, $XCo(DH)_2L$ (DH = monoanion of dimethylglyoxime), the simple B_{12} model shown in Scheme 1. The considerable amount of structural, spectroscopic, thermodynamic and kinetic data for a wide variety of X and L ligands has allowed study of trends in these properties in terms of the steric and electronic properties of the axial ligands X and L [15].

Weakening of the Co–C bond (steric *cis*-influence), as measured by its lengthening and by a decrease in bond dissociation energies, was essentially related to an increase in bulk of R, which sterically interacts with the DH ligands. However, a lengthening of this bond was also attributed to an increase of the electron donating ability of the X group [15]. Furthermore, the Co–X bond, especially with bulky X ligands, is lengthened by an increase in bulk of L which, forcing the $(DH)_2$ moiety to bend towards L, provokes a lengthening of the Co–L bond (steric *trans* influence).

When X is varied, a lengthening of the Co–L distance (electronic *trans*-influence) as well as an increase of several orders of magnitude in the rate constant (k) for the L displacement

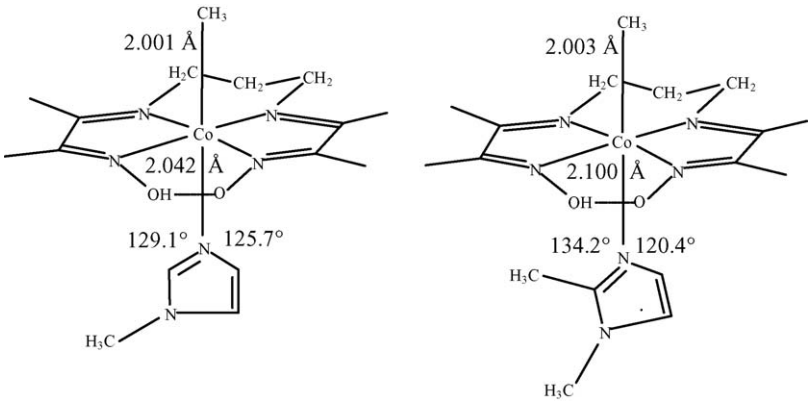

Scheme 2.

reaction (electronic *trans* effect) were found. On the other hand, an increase in the bulk of L determines the lengthening of the Co–L bond (steric *cis*-influence) and an increase of two orders of magnitude in *k* (steric *cis* effect).

Finally, when cobaloximes were compared with other Co(III) complexes having the same axial fragment, many of the chemical properties of the latter, such as the geometry, the spectroscopic properties and the kinetics, are significantly affected by the change in the equatorial ligand (*cis* influence and *cis* effect) [15].

The observation that in cobaloximes both axial distances Co–X and Co–L lengthen when the electron σ-donating ability of X increase has been called *inverse trans*-influence [60], in contrast with the *regular trans*-influence, which occurs when the Co–X bond shortens and the Co–L bond lengthens (see Section 4.3) [61].

4.3. *cis and trans effects in cobalamins*

Most conclusions derived for cobaloximes, described in Section 4.2, also qualitatively apply to cobalamins. However, significant quantitative differences, related to the variation of electronic nature of the Co centre, induced by the different equatorial moiety in the two systems, have been clearly established, as described below.

Inspection of Table 1 clearly shows that the electronic *trans*-influence exerted by X on the Co–NB3 distance provokes a lengthening of about 0.3 Å ongoing from the very weak electron donating H_2O ligand to the strong electron σ-donating *i*-amyl group. The Co–NB3 distance generally increases in the following order of the donor atom of the X ligand:

$$O < N < S < C.$$

Some years ago, a very good correlation ($r^2 = 0.990$) between the Co–NB3 bond length and K_{Co}, the equilibrium constant for coordination of benzimidazole to cobalt [62], was found for X = H_2O, CN, Me, Adepr, Ado [63]. This correlation (actually that between the free energy of the base-on formation, derived from K_{Co}, and the Co–NB3 bond length) is diminished when four additional cobalamins, more recently structurally characterized, were included [31]. However, the new correlation (Fig. 17) for nine cobalamins (X = H_2O, CN, CF_3, CHF_2, CH=CHCl, CH_2=CH, Me, Adepr, Ado), with $r^2 = 0.917$, becomes very good ($r^2 = 0.984$) when data points for the fluorinated cobalamins are omitted [31]. It should be noted that the corresponding structures of the fluorinated cobalamins are the least accurate structural determinations among those included in the correlation, as can be seen from the E.S.D.'s of their distances, given in parentheses in Table 1.

In the case of the alkylcobalamins (Table 1), the Co–NB3 distance increases with an increase in the electron donating ability of the alkyl group, although the CHF_2 group provokes a lengthening slightly greater than that of Me [64].

An example of steric *cis*-influence in cobalamins is furnished by comparison of the Co–NB3 distances in MeCbl (2.162(4) Å) and CNCbl (2.041(3) Å) with those of 2.09 and 1.968(9) Å in the the corresponding Cbl analogues, Co-β-methyl- [48] and Co-β-cyano-α-imidazolylcobamide [49], respectively, having the imidazole in place of the benzimidazole residue. As already observed, the decrease of about 0.07 Å in both Me and CN imidazolyl derivatives is ascribable to the smaller bulk of imidazole than that of the benzimidazole residue. The difference in bulk between the two residues is also reflected in the smaller

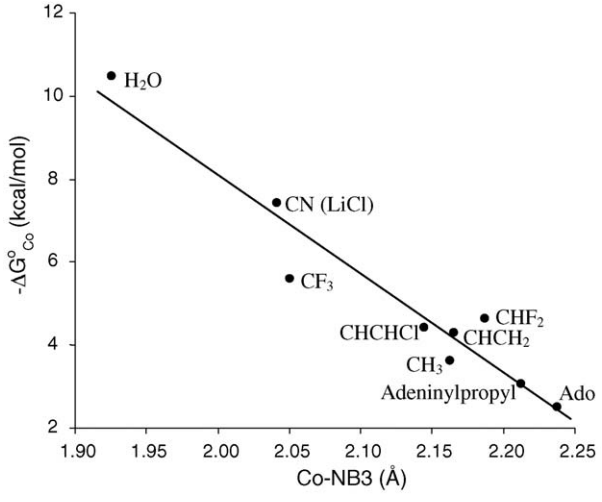

Fig. 17. Correlation between the Co—NB3 bond length and the free energy of formation of the base-on form of XCbl for several X axial ligands.

values of the fold angles of the equatorial ring in the imidazolyl compounds (cf. Section 3.2). This is in agreement with the finding that in $XCo(DH)_2L$, the Co–L distance increase in the order imidazole < py ≈ 1,3,5-trimethylbenzimidazole < 1,2-dimethylimidazole, for the same ligand X, in accordance with the bulk of L and not with its basicity [15].

The Co–C distances vary by about 0.15 Å, increasing with both the increasing bulk (steric *cis*-influence) and electron donating ability (electronic *cis*-influence) of X, as already found in cobaloximes [65]. In fact, the Co–C bond of 1.979(4) Å when X = Me, increases to 2.033(4) and 2.044(3) Å when X = Ado and *i*-amyl Ado (more bulky, but more electron donating groups than Me), respectively. It shortens to 1.88(1) and 1.949(8) Å when $X = CF_3$ and CHF_2, more electron withdrawing, but more bulky groups than Me. On the contrary, the Co–C bond length of 1.911(7) Å in (CH_2=CH)Cbl lengthens to 1.951(7) in (*cis*-CH=CHCl)Cbl, as a result of the steric repulsion between the *cis*-Cl and the equatorial ligand [31].

Resonance Raman spectroscopy for Me- and AdoCbl gave stretching frequencies, ν_{Co-C}, of 506 and 430 cm^{-1}, respectively [66]. A similar value of 500 cm^{-1} for crystalline MeCbl was obtained by Fourier Transform Raman spectroscopy [67]. The corresponding values of the Co–C bond dissociation enthalpy (BDE) towards homolysis have been reported to be 37 ± 3 and 30 ± 2 kcal/mol in MeCbl and AdoCbl, respectively [68]. The ν_{Co-C}, BDE and Co–C bond length values are consistent with a stronger Co–C bond in MeCbl than that in AdoCbl, although ab initio theoretical calculations [46a] on the whole cobalamin molecule, gave values of the bond order of 0.15 in the latter and of 0.13 in the former, which should be compared with that of 0.23 in CNCbl [46b].

Recent DFT calculations on simplified corrin model derivatives [32] have furnished values of the calculated Co–C BDE in vinyl- and *cis*-chlorovinyl cobalamins which are larger by about 7 kcal/mol than that calculated for MeCbl. In addition, a linear correlation between the calculated Co–C bond lengths and BDEs, similar to that observed in several alkylcobalamins [69], has been observed for variously chlorinated alkenylcobalamins. As expected, these correlations show that the BDE decreases with increasing Co–C distance. In the vinyl series, the calculated Co–C BDE decreases and the Co–C distance increases with increasing number of substituted Cl to such an extent that the Co–C BDE in the trichlorovinyl Cbl model is smaller and the Co–C distance is longer than that calculated in the MeCbl model. However, the increase in the calculated Co–C distances corresponds to a decrease in the calculated *trans* Co–NB3 distance. Therefore, these calculations do not support an inverse *trans*-influence in chlorovinylcobalamins [32].

4.4. Regular and inverse trans-influence in cobalamins

Contrary to the regular *trans*-influence, which occurs when the lengthening of one axial bond corresponds to a shortening of the other, in alkylcobalamins, as also occurs in alkylcobaloximes, both the axial distances lengthen or shorten when the electron donating ability of the X group increases or decreases, respectively [60]. Thanks to the more available data, this inverse *trans*-influence has been revisited for other cobalamins, not containing a Co–C bond [38,40].

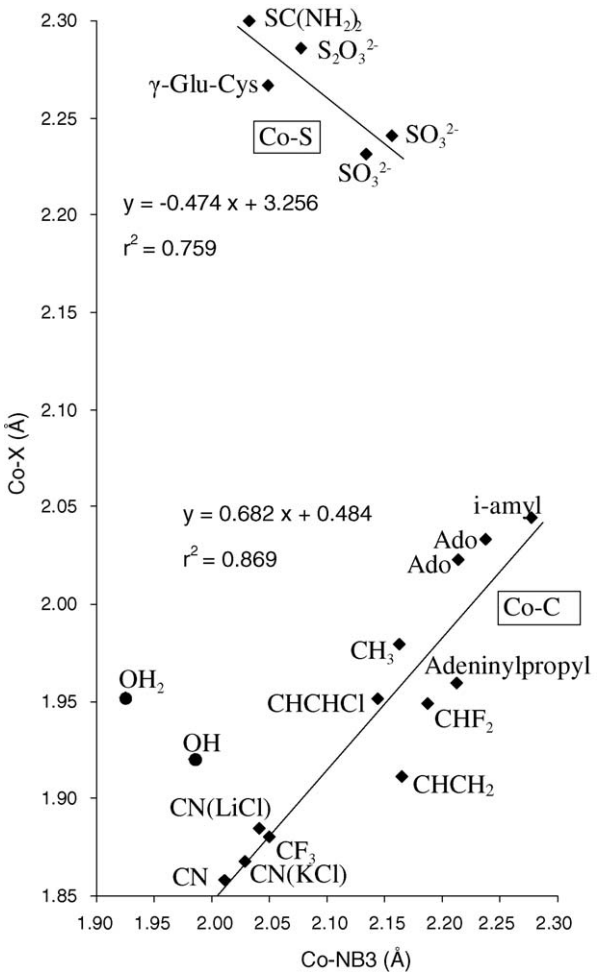

Fig. 18. Plot of the axial Co–S and Co–C distances vs. the Co–NB3 distances for several S— and C—Co bonded cobalamins, respectively. The equation and r^2 of each linear regression are given. Data points for H_2OCbl^+ and OHCbl are also indicated.

A useful way to analyze the regular and inverse *trans*-influence is to plot the Co–X distances, for X groups bonded to Co through the same donor atom, against the corresponding Co–NB3 distances. Using the data of Table 1, the two correlations for X groups having C and S donors are shown in Fig. 18. Similar correlations cannot be obtained for X groups containing either N or O donors, due to the lack of sufficient experimental data.

As expected, for cobalamins containing the Co–C bond the fairly good correlation ($r^2 = 0.87$) has a positive slope of 0.68, regardless of the C atom hybridization, confirming the presence of the inverse *trans*-influence. On the contrary, for the less numerous cobalamins containing the Co–S bond the fair correlation ($r^2 = 0.759$), has a negative slope of −0.47, giving an example of regular *trans*-influence [38,40]. The regular *trans*-influence in cobalamins has been further demonstrated by analysis of UV/vis spectra, namely the shift of the Cbl α, β and γ bands as a function of the Co–NB3 distance for $X = H_2O$, NO_2, S_2O_3, SeCN, SO_3 and Me [70].

A more accurate theoretical analysis of the inverse *trans*-influence in alkyl corrin model has concluded that it relies on an unusual combination of a poor σ/π base and a strong σ-donating alkyl group [71]. DFT calculations on the corrin model [40] have shown that, in the inverse *trans*-influence, the positive charge on Co increases with a lengthening of both the Co–C and Co–NB3 distances. Conversely, the positive charge on Co decreases with a lengthening of the Co–NB3 bond and increases with a lengthening of the Co–S bond. In fact, in the "regular" *trans*-influence, an increase in the electron σ-donation of the alkyl group is reflected in a decrease of the positive charge on cobalt. Therefore, the effect appears to be electronic in nature. On the other hand, in the "inverse" *trans*-influence the positive metal charge increases with the σ-donating power of the alkyl group. Thus, it cannot be only electronic, but it is also steric in nature, due to the large bulk of the σ-donating alkyl group. The steric repulsion, caused by the bulk of X, lengthens the Co–C bond (steric *cis*-influence), whereas the Co–NB3 bond is lengthened by electronic *trans*-influence and, consequently, the σ-donation from axial ligands to the metal decreases, leading to a more positive metal charge.

4.5. Comparison of cobalamins and cobaloximes

Comparison of the axial fragment features in cobalamins and cobaloximes has furnished useful insights into some of the metal properties in cobalamins [36,42].

4.5.1. The axial Co–N bond

Available axial distances in cobalamins (with E.S.D.'s < 0.01 Å) and $XCo(DH)_2L$ cobaloximes (L = pyridine (py)) [72] are compared in Table 1.

It was shown [42] that there is a fairly good linear relationship ($r^2 = 0.938$ with a slope of 2.00) between Co–py and Co–NB3 distances for several X groups, ranging from the very weak *trans* influencing H_2O to the strong *trans* influencing Ado. Inclusion of additional data (with E.S.D.'s < 0.01 Å) gives a very similar relationship, with $r^2 = 0.948$ and slope of 2.03, the plot being shown in Fig. 19. The slope of 2.03 indicates a much greater sensitivity of the Co–NB3 bond with respect to the Co–py bond in responding to the *trans* influence of X which is mediated by the equatorial ligand (i.e. the electronic *cis*-influence of the corrin nucleus noticeably differs from that of $(DH)_2$). Since the Co–NB3 distances in aquacobalamin and $H_2OCo(DH)_2py$ are very close, the *cis*-influence is predominantly electronic, in spite of the more bulky corrin ring. It should be noted that the Co–NB3 distance in CHF_2Cbl is slightly longer than that in MeCbl. This is unexpected since fluoroalkyl derivatives are supposed to have a significantly lower *trans* influence than that of the analogous alkyls, as it has been shown in simple B_{12} models [73].

4.5.2. The Co–X bond

The plot of the Co–X distances in cobalamins against those in cobaloximes (with E.S.D.'s < 0.01 Å) is reported in Fig. 20. This plot shows that the Co–X bond in cobalamins and cobaloximes responds in a similar way to steric and electronic effects. However, the point relative to CN falls significantly *below* the values

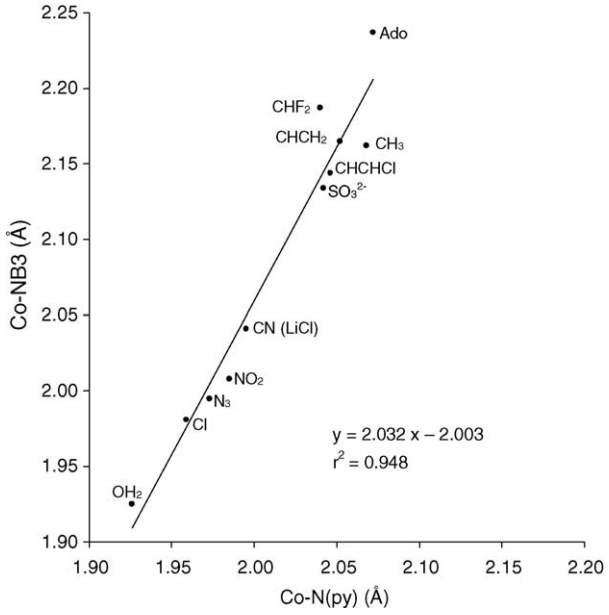

Fig. 19. Plot of the Co–NB3 distances in XCbl against Co–py in $XCo(DH)_2py$ with the equation and r^2 of the linear regression.

predicted by the correlation for the other groups. This strongly suggests that the π-back electron donation from Co to CN, shown to be appreciable in these systems by Brown et al. by means of ^{15}N and ^{13}C NMR measurements [74], is more enhanced in cyanocobalamin than in cyanocobaloxime. Such a difference can be structurally measured by the shortening of about 0.05 Å of the Co–C bond and by the lengthening of about 0.09 Å of the C–N bond from 1.077(3) Å in cyanocobaloxime [75] to 1.164(6) Å in the cyanocobalamin [42]. Analogously, the $\nu_{C\equiv N}$ in CNCbl is 2141.0 cm^{-1} [53], whereas it is 2132.0 cm^{-1} in $CNCo(DH)_2py$ [74b]. On the other hand, the points relative to Cl, N_3 and H_2O groups are all *above* the line in Fig. 20. In fact, the Co–X distances for *trans*-influencing ligands weaker

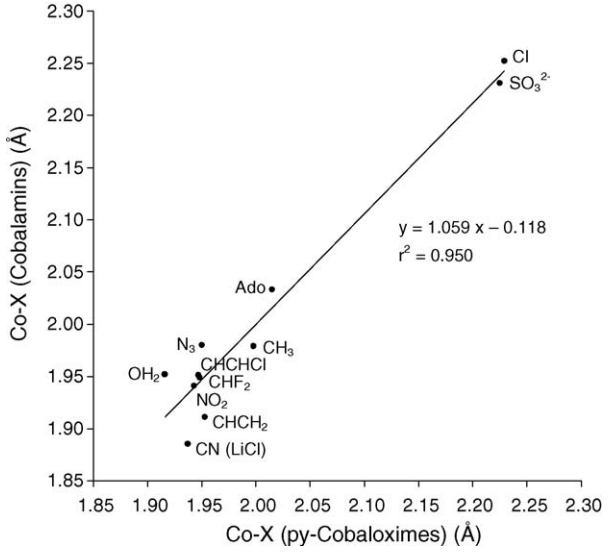

Fig. 20. Plot of the axial Co–X distances in XCbl vs. those in $XCo(DH)_2py$ with the equation and r^2 of the linear regression.

than benzimidazole, such as Cl, N_3 and H_2O, are lengthened in cobalamins with respect to cobaloximes, whereas for *trans*-influencing X ligands stronger than benzimidazole, the Co–X bond is almost unaffected. On the other hand, the greater electron richness of Co in cobalamins [42] enhances the π-back donation to CN with respect to cobaloximes, provoking the relative shortening of the Co–X distance. These observations clearly agree with the better transmission of the *trans*-influence in cobalamins than in cobaloximes. For this reason, if CN, Cl, N_3 and H_2O groups are excluded, the correlation improves significantly to $r^2 = 0.970$ with the following equation: Co–X (Cbl) = 1.06Co–X (cobaloxime) − 0.123. The point relative to vinyl is an outlier and it can be hypothesized that this is a consequence of the possible π-back donation from Co the vinyl ligand, more enhanced in cobalamins than in cobaloximes, as also occurs in the cyano derivative. The chlorovinyl derivative is not an outlier since this possible effect is compensated by the lengthening due to its bulk (see Section 4.3).

These structural and spectroscopic observations could represent a quantitative measure of the different behaviour of the cobalt centre in the two systems, due to the higher electronic charge put on the metal centre by the corrin ligand than that put by dimethylglyoximates. Available electrochemical data nicely agree with this view. In fact, the one electron reduction potential, $E_{1/2}$, for MeCbl was reported to be −1.60 V by Lexa and Saveant [76]. This value was confirmed by a subsequent work [77] which also reported a value of −1.38 V for neopentylcobalamin. The $E_{1/2}$ values for $XCo(DH)_2(Me_3Bzm)$, with X = Me and neo-pentyl are −1.45 and −1.27 V [42], respectively, remarkably shifted towards less negative values with respect to cobalamins.

Therefore, it may be concluded that the greater electron richness of Co in cobalamins on one hand enhances the π-back donation to CN with respect to cobaloximes and, on the other side, makes the transmission of the *trans* influence more effective in cobalamins, which can be detected by distance measurements.

4.6. The elusive nitrosocobalamin

Many years ago, Williams and co-workers [78] reported that the spectroscopic analysis indicated no formation of the complex nitrosocobalamin (NOCbl), when NO was reacted with either aquacobalamin or Cob(II)alamin, Vitamin B_{12r}. An analogous conclusion was reached about the formation of O_2Cbl. However, several years later the latter complex was obtained by solid state oxygenation of Vitamin B_{12r} and structurally characterized [79]. On the other hand, the pentacoordinated $NOCo(DH)_2$ analogue, an air sensitive product, has been synthesized and crystallographically characterized as bent nitrosyl derivative [80]. To our knowledge, this is the only example of a Co(III) pentacoordinated cobaloxime so far reported. Furthermore, the synthesis and the X-ray structure of several other Co(III) pentacoordinated bent nitrosyl complexes having delocalized equatorial ligands, such as porphyrin [81] or tetradentate Schiff bases (salen and acacen) [82], the latter being proposed as Vitamin B_{12} models [15b], have been reported. Finally, the X-ray structure of the six coordinate $[NOCo(NH_3)_5]^+$ cation has also been reported [83].

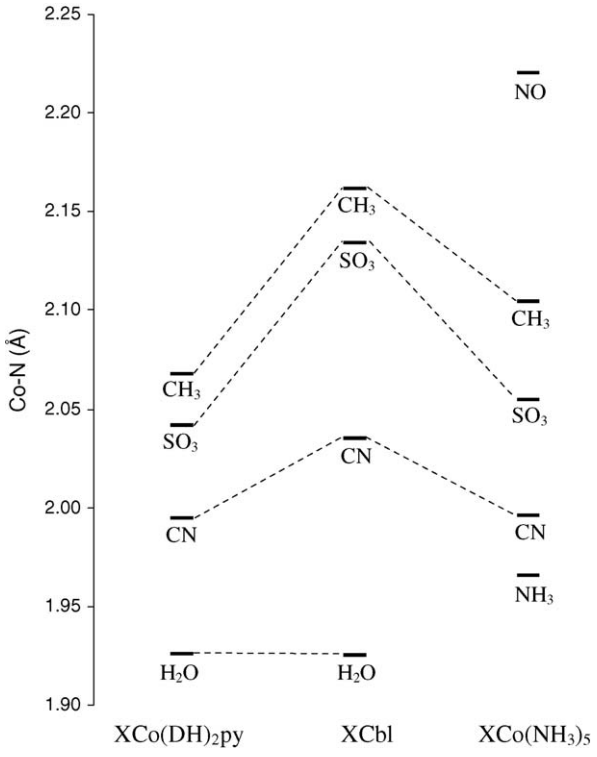

Fig. 21. Comparison of the axial Co—N bond lengths (E.S.D. < 0.005 Å) in $XCo(DH)_2py$, XCbl and $XCo(NH_3)_5$.

The above results allow us to speculate both about the possibility that Co in cobalamin may bind NO and about the geometry of the product. A comparison of very accurate axial Co–N bond lengths (E.S.D. < 0.005 Å) in $XCo(DH)_2py$, XCbl and $XCo(NH_3)_5$ is shown in Fig. 21. This figure illustrates a nice example of electronic *cis*-influence of the equatorial moiety in the order $(DH)_2 \leq (NH_3)_4 \ll$ Cbl. In penta-amino derivatives, it is apparent that a bent NO group exerts a strong *trans* influence, even stronger than that of Me. The strong *trans* influence ability of NO leads to the formation of the rare pentacoordinated cobaloxime [80]. This finding allows us to speculate about the NOCbl compound, by suggesting that it may be obtained through a synthetic procedure similar to that used for obtaining the cobaloxime analogue [80], probably in either base-off form or with a very long Co–NB3 distance.

5. Summary

The analysis of structural features of cobalamins allows interpretation of some properties of these biomolecules in the solid state and in solution. The crystal packing exhibits an interesting pattern principally ascribable to the inter and intra H-bond among the corrin side chains and the solvent molecules. Particularly, accurate knowledge of the geometry of the axial fragment allows the factors affecting the strength (and length) of the axial bonds to be established. This has biological relevance since the breaking and forming of these bonds is involved in the binding of Cbl to the apoproteins as well as in the catalytic mechanisms of Vitamin B_{12} based enzymes. Comparison to simple Cbl models,

the cobaloximes, allows formulation of qualitative hypotheses on the electronic nature of the cobalt centre in cobalamins.

Acknowledgement

This work was supported by MIUR (Rome, Italy), PRIN 2003037580.

References

[1] B. Kräutler, D. Arigoni, B.T. Golding (Eds.), Vitamin B_{12} and B_{12}-Proteins, Wiley–VCH, Weinheim, 1998.
[2] R. Banerjee (Ed.), Chemistry and Biochemistry of B_{12}, John Wiley & Sons, New York, 1999.
[3] D.H. Alpers, G.J. Russel-Jones, in: R. Banerjee (Ed.), Chemistry and Biochemistry of B_{12}, John Wiley & Sons, New York, 1999, p. 411ff.
[4] R.H. Allen, B. Seetharam, N.C. Allen, E.R. Podell, D.H. Alpers, J. Clin. Invest. 61 (1978) 1628.
[5] S. Bose, S. Seetharam, B. Seetharam, J. Biol. Chem. 270 (1995) 8152.
[6] E. Nexø, in: B. Kräutler, D. Arigoni, T. Golding (Eds.), Vitamin B_{12} and B_{12}-Proteins, Wiley–VCH, Weinheim, 1998, p. 461ff.
[7] J.F. Kolhouse, R.H. Allen, J. Clin. Invest. 60 (1977) 1381.
[8] J.M. Pratt, in: H. Sigel, A. Sigel (Eds.), Metal Ions in Biological Systems, vol. 29, Marcel Dekker Inc., New York, 1993, p. 229.
[9] L. Marzilli, in: J. Reedijk, E. Bouwman (Eds.), Bioinorganic Catalysis, Marcel Dekker Inc., New York, 1999, p. 423.
[10] J. Stubbe, S. Licht, G. Gerfen, S. Booker, in: R. Banerjee (Ed.), Chemistry and Biochemistry of B_{12}, John Wiley & Sons, New York, 1999, p. 320.
[11] R.G. Matthew, J.T. Drummond, Chem. Rev. 90 (1990) 1275.
[12] S.W. Ragsdale, M. Kumar, Chem. Rev. 96 (1996) 2519.
[13] P.G. Lenhert, D.C. Hodgkin, Nature 192 (1961) 937.
[14] M. Rossi, J.P. Glusker, L. Randaccio, M.F. Summers, P.J. Toscano, L.G. Marzilli, J. Am. Chem. Soc. 107 (1985) 1729.
[15] (a) L. Randaccio, Comments Inorg. Chem. 21 (1999) 327;
(b) L. Randaccio, N. Bresciani-Pahor, E. Zangrando, L.G. Marzilli, Chem. Soc. Rev. 18 (1989) 225.
[16] F. Mancia, N.H. Keep, A. Nakagawa, P.F. Leadlay, S. McSweeney, B. Rasmussen, P. Bösecke, O. Diat, P.R. Evans, Structure 4 (1996) 339;
F. Mancia, P.R. Evans, Structure 6 (1998) 711.
[17] Y. Zhao, P. Such, J. Retey, Angew. Chem. Int. Ed. 31 (1992) 215.
[18] G. Marzilli, M.F. Summers, N. Bresciani-Pahor, E. Zangrando, J.P. Charland, L. Randaccio, J. Am. Chem. Soc. 107 (1985) 6880.
[19] M. Dixon, S. Huang, R.G. Matthews, M.L. Ludwig, Structure 4 (1996) 1263;
C. Drennan, S. Huang, J.T. Drummond, R.G. Matthwes, M.L. Ludwig, Science 266 (1994) 1669.
[20] N. Shibata, J. Masuda, T. Tobimatsu, T. Toraya, K. Suto, Y. Morimoto, N. Yasuoka, Structure 7 (1999) 997.
[21] (a) K.L. Brown, Chem. Rev. 105 (2005) 2075;
(b) C.B. Perry, H.M. Marques, S.A.J. Sci. 100 (2004) 368.
[22] H.P. Chen, S.H. Wu, Y.L. Li, C.M. Chen, S.S. Tsay, J. Biol. Chem. 276 (2001) 44744.
[23] J. Masuda, N. Shibata, Y. Morimoto, T. Toraya, N. Yasuoka, Structure 8 (2000) 775;
V.P. Bandarian, G.H. Reed, Biochemistry 41 (2002) 8580;
C.C. Lawrence, G.J. Gerfen, R. Nitsche, M.J. Robins, J. Retey, J. Stubbe, J. Biol. Chem. 274 (1999) 7039;
M.D. Sintchak, G. Aryara, B.A. Kellog, J. Stubbe, C.L. Drennan, Nat. Struct. Biol. 9 (2002) 293.
[24] S.N. Fedosov, L. Berglund, E. Nexø, T.E. Petersen, J. Biol. Chem. 274 (1999) 26015;
S.N. Fedosov, N.U. Fedosova, E. Nexø, T.E. Petersen, J. Biol. Chem. 275 (2000) 11791;
S.N. Fedosov, L. Berglund, N.U. Fedosova, E. Nexø, T.E. Petersen, J. Biol. Chem. 277 (2002) 9989.
[25] Unpublished results from this laboratory.
[26] (a) H. Savage, Biophys. J. 50 (1986) 947;
(b) P.B. Bouchiere, J. Finney, H.F.J. Savage, Acta Cryst. B50 (1994) 566.
[27] G. Wohlfart, G. Diekert, in: R. Banerjee (Ed.), Chemistry and Biochemistry of B_{12}, John Wiley & Sons, New York, 1999, p. 871ff.
[28] R.E. Doherty, Environ. Forensics 1 (2000) 69;
P.J. Squillace, M.J. Moran, W.W. Lapham, C.V. Price, R.M. Clawges, J.S. Zogorski, Environ. Sci. Technol. 33 (1999) 4176.
[29] C. Holliger, G. Wohlfarth, G. Diekert, FEMS Microbiol. Rev. 22 (1998) 383.
[30] D.R. Burris, C.A. Delcomyn, B.L. Deng, L.E. Buck, K. Hatfield, Environ. Toxicol. Chem. 17 (1998) 1681;
M. Semadeni, P.C. Chiu, M. Reinhard, Environ. Sci. Technol. 32 (1998) 1207, and references therein.
[31] K.M. McCauley, D.A. Pratt, S.R. Wilson, J. Shey, T.J. Burkey, W.A. van der Donk, J. Am. Chem. Soc. 127 (2005) 1126.
[32] D.A. Pratt, W.A. van der Donk, J. Am. Chem. Soc. 127 (2005) 384.
[33] K. Gruber, G. Jogl, G. Klintscher, C. Kratky, in: B. Kräutler, D. Arigoni, B.T. Golding (Eds.), Vitamin B_{12} and B_{12}-Proteins, Wiley–VCH, Weinheim, 1998, p. 335ff.
[34] C. Kratky, B. Kräutler, in: R. Banerjee (Ed.), Chemistry and Biochemistry of B_{12}, John Wiley & Sons, New York, 1999, p. 9ff.
[35] H.M. Marques, K.L. Brown, Coord. Chem. Rev. 225 (2002) 123.
[36] L. Randaccio, S. Geremia, G. Nardin, M. Slouf, I. Srnova, Inorg. Chem. 38 (1999) 4087.
[37] D.C. Hodgkin, J. Lindsay, R.A. Sparks, K.N. Trueblood, J.G. White, Proc. R. Soc. London A266 (1962) 494.
[38] G. Garau, S. Geremia, L.G. Marzilli, G. Nardin, L. Randaccio, G. Tauzher, Acta Cryst. B59 (2003) 51.
[39] L. Randaccio, M. Furlan, S. Geremia, M. Slouf, Inorg. Chem. 37 (1998) 5390.
[40] L. Randaccio, S. Geremia, M. Stener, D. Toffoli, E. Zangrando, Eur. J. Inorg. Chem. (2002) 93.
[41] T.L.C. Hsu, N.E. Brasch, R.G. Finke, Inorg. Chem. 37 (1998) 5109.
[42] L. Randaccio, M. Furlan, S. Geremia, M. Slouf, I. Srnova, D. Toffoli, Inorg. Chem. 39 (2000) 3403.
[43] N.E. Brash, F. Muller, A. Zahl, R. van Eldik, Inorg. Chem. 33 (1998) 4891;
N.E. Brash, M.S.A. Hamza, R. van Eldik, Inorg. Chem. 33 (1998) 3216, and references therein.
[44] D.C. Hodgkin, in: B. Zagalak, W. Friedrich (Eds.), Vitamin B12, Walter Gruyter, Berlin, 1979, p. 19.
[45] J.P. Glusker, in: D., Dolphin, (Ed.), B12, vol. I, John Wiley & Sons, New York, 1981, p. 23.
[46] (a) L. Ouyang, P. Rulis, W.Y. Ching, G. Nardin, L. Randaccio, Inorg. Chem. 43 (2004) 1235;
(b) E.Z. Kurmaev, A. Moewes, L. Ouyang, L. Randaccio, P. Rulis, W.Y. Ching, M. Bach, M. Neumann, Europhys. Lett. 62 (2003) 582;
L. Ouyang, L. Randaccio, P. Rulis, E.Z. Kurmaev, A. Moewes, W.Y. Ching, J. Mol. Struct. (Theochem) 622 (2003) 221.
[47] L. Ouyang, P. Rulis, W.-Y. Ching, M. Slouf, G. Nardin, L. Randaccio, Spectrochim. Acta A 61 (2005) 1647.
[48] B. Kräutler, R. Konrat, E. Stupperich, G. Färber, K. Gruber, C. Kratky, Inorg. Chem. 33 (1994) 4128.
[49] M. Fasching, W. Schmidt, B. Kräutler, E. Stupperich, A. Schmidt, C. Kratky, Helv. Chim. Acta 83 (2000) 2295.
[50] C.B. Perry, M.A. Fernandes, H.M. Marques, Acta Cryst. C60 (2004) m165.
[51] R.K. Suto, N.E. Brasch, O.P. Anderson, R.G. Finke, Inorg. Chem. 40 (2001) 2686.
[52] C. Kratky, G. Färber, K. Gruber, Z. Deuter, H.F. Nolting, R. Konrat, B. Kräutler, J. Am. Chem. Soc. 117 (1995) 4654.
[53] J.M. Pratt, in: R. Banerjee (Ed.), Chemistry and Biochemistry of B_{12}, John Wiley & Sons, New York, 1999, p. 73ff.
[54] E.B. Stasrikov, T. Stener, Acta Cryst. B54 (1998) 94.
[55] M. Tollinger, R. Konrat, B. Kräutler, Helv. Chim. Acta 82 (1999) 158.
[56] K.L. Brown, H.M. Marques, J. Mol. Struct. (Theochem) 453 (1998) 209.

[57] E.M. Scheuring, I. Sagi, M.R. Chance, Biochemistry 33 (1994) 6310;
M.R. Chance, in: R. Banerjee (Ed.), Chemistry and Biochemistry of B_{12}, John Wiley & Sons, New York, 1999, p. 43ff.
[58] F. Champloy, K. Gruber, G. Jogl, C. Kratky, J. Synchrotron Radiat. 7 (2000) 267;
F. Champloy, G. Jogl, R. Reitzer, W. Buckel, H. Bothe, B. Beatrix, G. Broeker, A. Michaolowicz, W. Meyer-Klaucke, C. Kratky, J. Am. Chem. Soc. 121 (1999) 11780.
[59] R. Reitzer, K. Gruber, G. Jogl, U.G. Wagner, H. Bothe, W. Buckel, C. Kratky, Structure 7 (1999) 891.
[60] D.J.A. De Ridder, E. Zangrando, H.B. Burgi, J. Mol. Struct. 374 (1996) 63.
[61] (a) M. Kita, K. Kashiwabara, J. Fujita, Bull. Chem. Soc. Jpn. 61 (1988) 3187;
(b) O. Foss, K. Maartmann-Moe, Acta Chem. Scand. Ser. A 41 (1987) 121;
N. Yoshinaga, N. Ueyama, T. Okamura, N. Nakamura, Chem. Lett. (1990) 1655;
D. Boström, R. Strandberg, N. Norén, Å. Oskarsson, Acta Cryst. C47 (1991) 2101.
[62] K.L. Brown, S. Peck-Siler, Inorg. Chem. 27 (1988) 3548.
[63] K.L. Brown, D.R. Evans, J.D. Zubkowski, E.J. Valente, Inorg. Chem. 35 (1996) 415.
[64] T. Wagner, C.E. Afshar, H.L. Carell, J.P. Glusker, U. Englert, H.P.C. Hogekamp, Inorg. Chem. 38 (1999) 1784.
[65] L. Randaccio, S. Geremia, E. Zangrando, C. Ebert, Inorg. Chem. 33 (1994) 4641.
[66] S. Dong, R. Padmakumar, R. Banerjee, T.G. Spiro, J. Am. Chem. Soc. 121 (1999) 7063, and references therein.
[67] S. Nie, P.A. Marzilli, L.G. Marzilli, N.T. Yu, J. Chem. Soc. Chem. Commun. (1990) 770.
[68] B.M. Martin, R.G. Finke, J. Am. Chem. Soc. 114 (1992) 585.
[69] T. Andriunov, M.Z. Zgierski, P.M. Kozlowski, J. Am. Chem. Soc. 123 (2001) 2679.
[70] C.B. Perry, M.A. Fernandes, K.L. Brown, X. Zou, E.J. Valente, H.M. Marques, Eur. J. Inorg. Chem. (2003) 2095.
[71] T. Andriunov, J. Kuta, M.Z. Zgierski, P.M. Kozlowski, Chem. Phys. Lett. 410 (2005) 410.
[72] The py series was chosen because of the larger amount of data available for comparison. This comparison should also be valid for cobaloximes with L = 1,5,6-trimethylbenzimidazole (Me3Bzm), since it has been shown [65] that the axial Co–X and Co–N distances are very close for both the L ligands and a large number of X groups. The Co–py distances for $X = SO_3$ and CHF_2, experimentally not available, have been calculated according to Ref. [36].
[73] S. Geremia, L. Randaccio, E. Zangrando, Gazz. Chim. Ital. 122 (1992) 229.
[74] (a) K.L. Brown, B.D. Gupta, Inorg. Chem. 29 (1990) 3854;
(b) K.L. Brown, S. Satyanarayana, Inorg. Chem. 31 (1992) 1366.
[75] W.M. Attia, E. Zangrando, L. Randaccio, L. Antolini, C. Lopez, Acta Cryst. C45 (1989) 1500.
[76] D. Lexa, J.M. Saveant, J. Am. Chem. Soc. 100 (1978) 3220.
[77] R.E. Sheperd, S. Zhang, P. Dowd, G. Choi, B. Wick, S. Choi, Inorg. Chim. Acta 174 (1990) 249.
[78] R.A. Firth, H.A.O. Hill, J.M. Pratt, R.G. Thorpe, R.J.P. Williams, J. Chem. Soc. (A) (1969) 381.
[79] E. Hohenester, C. Kratky, B. Kräutler, J. Am. Chem. Soc. 113 (1991) 4523.
[80] U. Englert, J. Strahle, Gazz. Chim. Ital. 118 (1988) 845.
[81] K.M. Kadish, Z. Ou, X. Tan, T. Boschi, D. Monti, V. Fares, P. Tagliatesta, J. Chem. Soc. Dalton Trans. (1999) 1595.
[82] K.J. Haller, J.H. Enemark, Acta Cryst. B34 (1978) 102;
P.A. Duffin, L.F. Lakworthy, J. Mason, A.N. Sheperd, R.M. Thompson, Inorg. Chem. 26 (1987) 2034.
[83] C.S. Pratt, B.C. Coyle, J.A. Ibers, J. Chem. Soc. (A) (1971) 2146.
[84] X. Zou, K.L. Brown, Inorg. Chim. Acta 267 (1998) 305.
[85] K.M. McCauley, S.R. Wilson, W.A. van der Donk, Inorg. Chem. 41 (2002) 393.
[86] S.M. Chemaly, H.M. Marques, C.B. Perry, Acta Cryst. C60 (2004) m88.
[87] T.G. Pagano, L.G. Marzilli, M.M. Flocco, C. Tsai, H.L. Carrell, J.P. Glusker, J. Am. Chem. Soc. 113 (1991) 531.